UDC 621.315.592

Dedicated to the blessed memory of the pioneers of amorphous semiconductors B.T. Kolomiets and N.A. Goryunova

Chalcogenide vitreous semiconductors in memory and information processing devices (Review)

© A.V. Kolobov[1,2], P.I. Lazarenko[3,2]

[1] Institute of Physics, Herzen State Pedagogical University of Russia,
191186 St. Petersburg, Russia
[2] Research Institute of Physical Studies, Herzen State Pedagogical University of Russia,
191186 St. Petersburg, Russia
[3] Laboratory „Materials and Devices of Active Photonics“,
National Research University MIET,
124498 Moscow, Zelenograd, Russia
E-mail: akolobov@herzen.spb.ru

Received November 9, 2025
Revised November 17, 2025
Accepted November 17, 2025

The discovery in 1955 of the semiconducting properties of chalcogenide glasses by B.T. Kolomiets and N.A. Goryunova started the era of amorphous semiconductors. The present review focuses on phase-change chalcogenides, which are now widely used in data recording and processing devices. After a historical introduction, the structure and properties of these materials are discussed, as well as current views on the mechanism of reversible phase transformations between the amorphous and crystalline states and the nature of the property contrast between them. This is followed by a description of commercial implementations of phase-change materials in optical and electronic non-volatile memory devices. The review concludes with a discussion of current trends in research and applications of phase-change chalcogenides, in particular, in 3D XPoint memory devices based on the Ovshinsky threshold switching effect, as well as in electronic and photonic neuromorphic networks.

Keywords: Chalcogenide vitreous semiconductors, phase-change materials, memory effect, Ovshinsky threshold switching, optical discs, non-volatile electronic memory, 3D XPoint memory, neuromorphic networks.

DOI: 10.61011/SC.2025.09.62832.8784

1. Introduction

The year 2025 marked the 70th anniversary of the discovery of the semiconductor properties of chalcogenide glasses by B.T. Kolomiets and N.A. Goryunova (Figure 1) at A.F. Ioffe Physical-Technical Institute of the USSR Academy of Sciences [1]. This discovery marked a rethinking of the nature of the band gap in semiconductors and marked the beginning of the era of amorphous semiconductors. A class of glasses with semiconductor properties has been named chalcogenide vitreous semiconductors (ChVS). About 20 years later, Sir N.F. Mott, who received the Nobel Prize for his studies in the field of amorphous semiconductors, noted in his Nobel speech that „band gap is a sophisticated concept, entirely dependent on quantum mechanics, and introduced for solids in the 1930's by the pioneering work of Bloch, Peierls and A.H. Wilson. The theory was based on the assumption that the material was crystalline ... Our curiosity was stimulated by the investigation of the Leningrad school under Kolomiets“ [2].

Subsequent experiments have shown that ChVSs are *p*-type semiconductors and are resistant to doping [3], as a result of which practical interest in these materials, as materials of modern and future electronics, has somewhat decreased, giving way to another amorphous semiconductor — hydrogenated amorphous silicon. In those years, it was hard to imagine that half a century later, ChVS would occupy one of the top positions in the list of materials used in memory devices and actively researched for applications in neuromorphic networks.

After the discovery of the semiconductor properties of ChVS, the cornerstone in the formation of amorphous chalcogenides was the results of research by Stanford Ovshinsky (Figure 2). Ovshinsky discovered that chalcogenide glasses of a certain composition exhibit a switching

Figure 1. B.T. Kolomiets and N.A. Goryunova – discoverers of amorphous semiconductors.

Figure 2. S.R. Ovshinsky, whose pioneering work led to the rapid development of memory elements on amorphous chalcogenides, in the office of his Institute for Amorphous Research a few days before his 90th birthday.

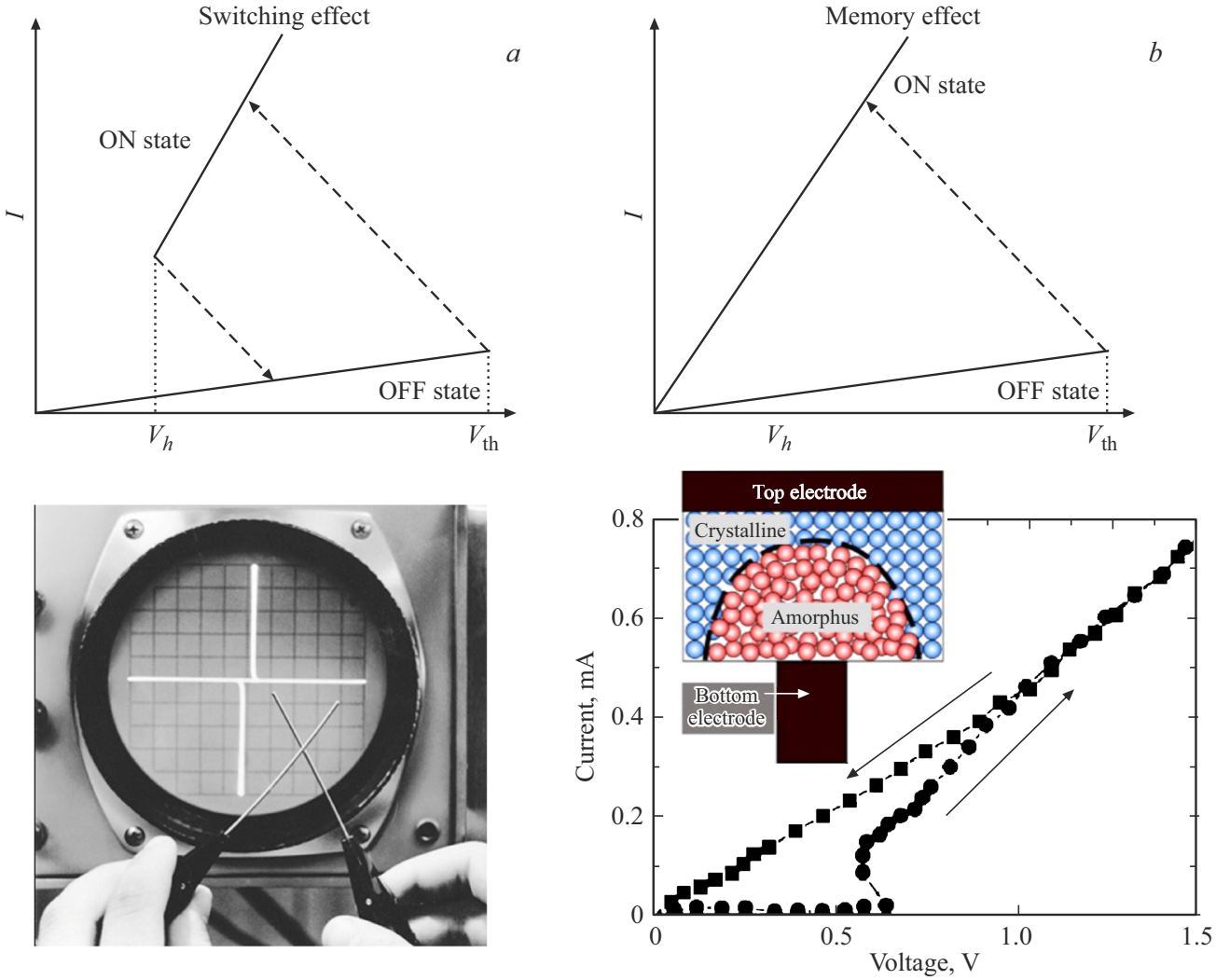

Figure 3. Switching (*a*) and memory effect (*b*). Bottom left — photo of Ovshinsky's original experiment, on the right — volt-ampere characteristic of the memory cell.

effect, namely, when an electric field of a certain magnitude is applied, they undergo an abrupt transition from a high-resistance state to a low-resistance state. After reducing the applied voltage below a certain value, the material reverts to its original state. Schematically, this process, known as the Ovshinsky threshold switching (OTS), is shown in Figure 3, *a*. At the same time, glasses of some other compositions remained in the low-resistance state even after the voltage was completely removed (Figure 3, *b*), i. e. they had a memory effect. Subsequent experiments have shown that during the transition to a low-resistance state, crystallization of the material takes place in materials with a memory effect. Later, this class of chalcogenides was called Phase-Change Materials (PCMs).

The above results were described in Ovshinsky's seminal paper published in Physical Review Letters in 1968 [4]. This article, which became one of top 5 most cited Physical Review Letters articles, has an interesting history. A month after it was submitted, Ovshinsky received a letter from the editor saying that the article had been sent for review and both reviewers recommended that it be rejected. But, the as the editor wrote further, „I liked the work, and I decided to publish it" [5]. This was how the first obstacle to the widespread practical use of phase-change materials was overcome.

Ovshinsky expected his discovery to be met with enthusiasm by his fellow physicists, but it was exactly the opposite. This is what Professor Helmut Fritzsche, Ovshinsky's friend and associate, who for many years headed the Department of Physics at the University of Chicago, told about it at the celebration dedicated to the 90th anniversary of Ovshinsky. „What a disappointment! Stan's discoveries were contemptuously dismissed and attacked by mainstream physicists. . . . Since his enemies were from the established research institutions, they were able to block all federal research support . . . " [6]. That's how it all started . . .

Figure 4. One of the authors (A.V. Kolobov) of this review at Stanford Ovshinsky's Institute for Amorphous Studies.

To continue his research Ovshinsky estabished at his own expense the Institute for Amorphous Studies. Famous scientists and Nobel laureates such as Sir Neville Mott, Isidore Rabi, Robert Wilson, Edward Teller, and Linus Pauling were guests of the Institute at various times. One of the authors of this review was also fortunate to visit this Institute on several occasiona (Figure 4). In the years following the publication of Ovshinsky's pioneering article, significant progress has been made in understanding the reversible crystallization-amorphization process of phase-change chalcogenides and its practical application [7–9]. At the same time, the OTS switching process has been studied much less intensively, and there is still no definitive understanding of the physics of this process. However, the studies of the switching effect has gained new momentum in the last few years.

This review presents a modern view of the structure and structural transformations occurring as a result of various impacts on phase-change semiconductors, the most dynamically developing class of chalcogenide glassy semiconductors, and highlights recent advances in the field of phase-change materials and their uses in the field of electrical and optical information storage and processing devices.

2. Structure of phase-change chalcogenides and the mechanism of phase transformations

The operational principle of phase-change materials is the following. The structure of the material in the solid phase depends on the cooling rate of the melt. In the case of slow cooling of the melt, in which the atoms can to occupy positions corresponding to the minimum energy during the cooling process, a crystal is obtained. During rapid cooling, at some point in time, the viscosity of the melt increases so that the atomic positions „freeze" resulting in a supercooled liquid and then a glassy (amorphous) phase. On the other hand, if the amorphous phase is heated to the crystallization temperature, it transforms to an ordered (crystalline) state. Thus, by varying the duration and temperature of heating and subsequent cooling, it is possible to reversibly transfer the material from the amorphous phase to the crystalline phase and vice versa (Figure 5, *a*).

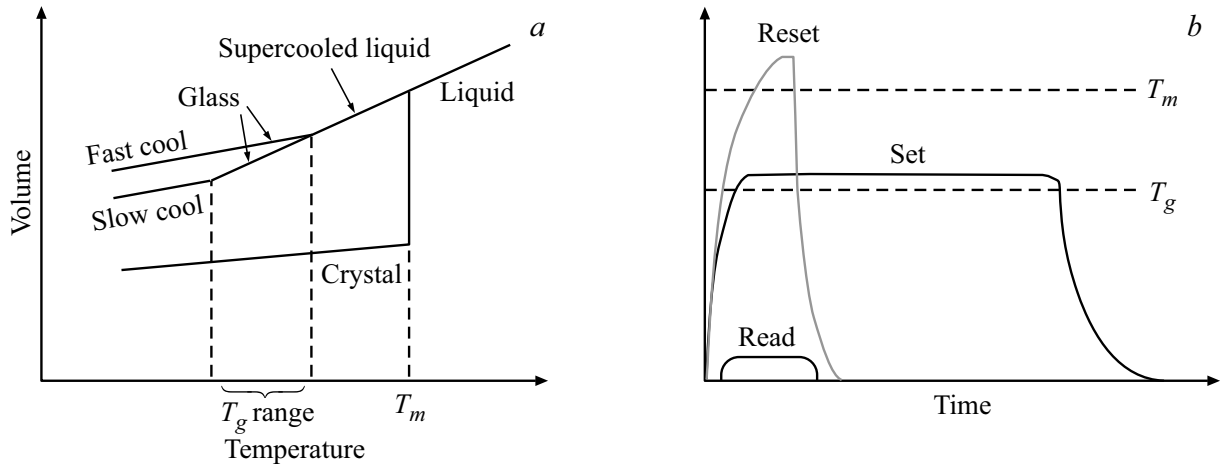

Figure 5. Scheme for obtaining crystalline and amorphous states upon cooling of the melt (*a*). Conversion of a phase-change material to amorphous (RESET) and crystalline (SET) states by pulses of different intensity (*b*).

In device structures, heating is carried out by laser pulses or current pulses (due to Joule heating). A short powerful pulse leads to melting of the material and its subsequent quenching into the amorphous phase (RESET state). High cooling rates are provided by the structure of the device, in particular in optical disks by the presence of a metal layer providing an effective heat sink. A pulse of lower intensity but longer duration allows the amorphous region to crystallize (SET state). Finally, low-intensity light is used for reading, which does not lead to a significant increase in temperature in the programmable area (Figure 5, *b*).

While the processes described above can hypothetically be implemented in many materials, for their practical use in memory devices, the material must simultaneously possess a set of various properties: (i) a significant contrast of properties between amorphous and crystalline states, (ii) stability of both states, (iii) rapid transition between the states, (iv) a sufficiently large number of switching cycles and a number of other properties. Materials that meet these requirements, as noted above, are commonly referred to as phase-change materials.

The second of these requirements implies a high energy barrier between the two states, while the implementation of the third requirement requires, on the contrary, a low barrier. Studies have shown that these conditions are met by glasses produced by cooling the so-called fragile liquids, in which the activation energy of viscosity depends on temperature. It was demonstrated in Ref. [10] using differential scanning calorimetry with ultrahigh cooling rates, that phase-change chalcogenides belong to this category.

Development of rewritable optical discs by Matsushita was the first breakthrough in the practical application of ChVS as memory materials. As a result of many years of research, compounds of the Ge–Sb–Te (GST) system, primarily those located along the $GeTe–Sb_2Te_3$ quasi-binary tie-line were recognized as optimal materials [11,12] and DVD-RAM rewritable optical compact discs based on them were introduced in the market in 2000. An alternative phase-change material Ag–In–Sb–Te (AIST) was proposed by Ricoh [13] and was used in CD-RW. From the user's point of view, there is not much difference between RAM and RW discs. From a materials science point of view, the difference is that the crystallization rate of GST is determined by the nucleation rate, while AIST is determined by the growth rate of crystalline nuclei.

Why did these materials turn out to be optimal? The properties of a material are known to be determined by its structure, which is more than clearly indicated by the name of a recent review „If you want to understand the functionality, study the structure" [14]. Naturally, first of all, the researchers studied the structure of the crystalline phase.

2.1. Crystalline phase

The structure of crystalline materials is usually studied by diffraction, when, based on the position and intensity of the Bragg peaks, the interplane distances in the crystal and then its atomic structure are determined. Applying this approach to the $Ge_2Sb_2Te_5$ (GST225) material, it was concluded that the crystalline phase has a rock-salt type lattice with a lattice parameter of 6.02 Å, in which 20 % of the cationic sites are vacant [15,16].

However, it should be borne in mind that traditional X-ray diffraction analysis is an averaging method and, as a result, is insensitive to local distortions of the structure [17,18], which was clearly demonstrated during the study of one of the end points of the quasi-binary tie-line — GeTe. Being very simple structurally and compositionally, GeTe is extremely multifunctional. It is a semiconductor and a high-pressure superconductor [19], a ferroelectric with only two atoms in its unit cell [20], a material with a record-breaking Rashba effect [21,22], and one of the best thermoelectrics [23]. However, the discussion of such multifunctionality of germanium telluride is beyond the

scope of this review, and here we will consider only those of its features that are important for its use as a phase-change material.

In the temperature range of interest, GeTe has a rhombohedral structure (space group $R3m$) [24], which can be viewed as a distorted rock-salt structure in which there are three short (~ 2.83 Å) and three long (~ 2.15 Å) Ge–Te bonds, and valence angles differ slightly from 90°. It is also interesting to note that although the stoichiometric GeTe formula is used to describe this composition, implying the same number of cations and anions, the composition of real crystals is almost always shifted towards tellurium and has $\sim 5\%$ vacancies on germanium sites, even in the case of crystallization of an amorphous film of stereometric composition [25]. The presence of germanium vacancies is due to the low energy of formation of such defects and may be the cause of the p-type conductivity of germanium telluride [26]. As the temperature increases, GeTe transforms into a paraelectric phase, the structure of which, based on experiments on neutron diffraction [27], was determined as a cubic rock-salt structure (Figure 6). A similar result was obtained using X-ray diffraction. Despite the fact that this result is well-known and often cited, the situation turned out to be somewhat more complicated, as was shown by studies of the local structure [28–30].

To study the local structure, X-ray absorption spectroscopy (X-ray absorption fine structure (XAFS) spectroscopy) and X-ray diffraction analysis taking into account the information between Bragg peaks, the so-called pair-distribution function (pdf) analysis [31] are most often used. In connection with the above, we note that in the traditional analysis of X-ray diffraction, the information between the Bragg peaks is considered the background and is subtracted from the spectrum before the main analysis is performed.

The essence of the XAFS method in the most general terms is as follows. When an X-ray photon with energy above the absorption edge is absorbed, a photoelectron wave is generated. Propagating through a solid, this wave is scattered on the atoms of the nearest environment. The scattered wave interferes with the outgoing wave, resulting in oscillations in the absorption spectrum above

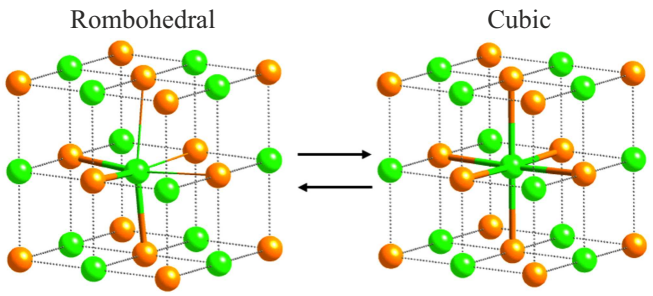

Figure 6. The structure of the ferroelectric (rhombohedral) GeTe (left) and the proposed cubic structure (right) for the paraelectric phase.

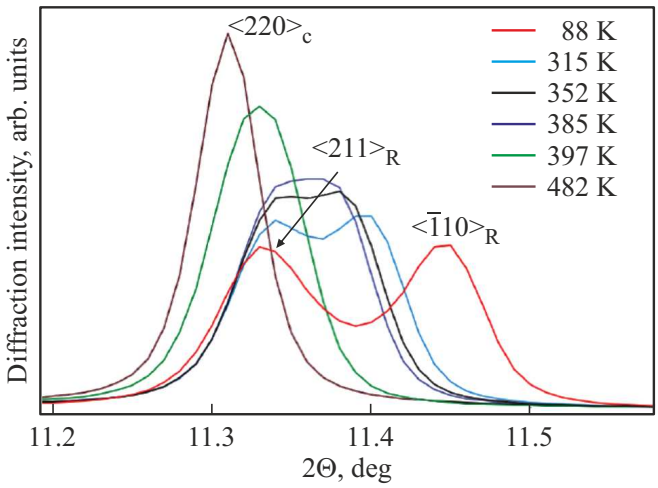

Figure 7. Temperature evolution of diffraction peaks of $Ge_8Sb_2Te_{11}$, the interpretation of which suggests the transition of the material from the rhombohedral phase to cubic [28].

the absorption edge. These oscillations are called the extended fine structure of X-ray absorption (extended X-ray absorption fine structure, EXAFS) [32].

From the analysis of the EXAFS spectra, complete information is obtained about the local structure around atoms of a certain type (the absorption edge of which is being studied), namely, the chemical nature of the nearest neighbors, their number (coordination number), distances to the nearest neighbors, and the degree of disorder in bond lengths. The latter value, by analogy with the analysis of X-ray diffraction spectra, is sometimes called the Debye-Waller factor. The main advantage of the method is its applicability to both ordered (crystalline) and disordered (amorphous) substances. Studies of the absorption edges of various elements included in the material, followed by synchronous analysis, allow one to obtain complete information about its local structure.

Figure 7 shows X-ray diffraction pattern obtained at different temperatures for the crystalline phase of $Ge_8Sb_2Te_{11}$ (the material used in Blu-ray discs), from which it can be seen that the splitting of the diffraction peaks characteristic of the rhombohedral phase disappears with increasing temperature, which was logically interpreted as a transition to the cubic phase [28].

At the same time, studies of the structure of GeTe and germanium-rich GST using EXAFS have unequivocally demonstrated that during the transition from the ferroelectric to the paramagnetic phase, the short and long bonds are preserved (Figure 8), i.e. locally, the material retains the characteristics of the rhombohedral phase [28,29]. This conclusion was also confirmed by experiments using the pdf-analysis [30]. The results obtained led to the conclusion that the ferroelectric-paraelectric transition is an order-disorder transition, when the distribution of short and long bonds changes from ordered to stochastic (Figure 9). In

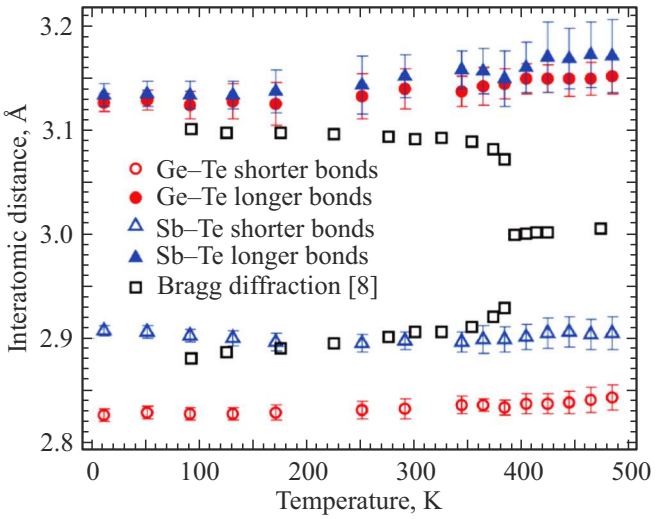

Figure 8. Temperature dependence of the Ge−Te and Sb−Te bond lengths in $Ge_8Sb_2Te_{11}$ obtained from Bragg diffraction and EXAFS spectra. In the ferroelectric-paraelectric transition region, the long and short Ge−Te and Sb−Te bonds are preserved, i. e. locally, the material retains the characteristics of the rhombohedral phase [28].

this case, Bragg diffraction should correspond to a cubic (on average) crystal.

Studies of the classical phase-change material, GST225, using EXAFS have shown that in the range of operating temperatures, the crystalline phase is not cubic, as assumed on the basis of early experiments on Bragg diffraction. It was shown that the nearest Ge−Te distances were ~ 2.83 Å, i. e., the same as in the binary GeTe and significantly larger than the sum of the covalent radii of the constituent elements ($R_{Ge} = 1.20$ Å, $R_{Te} = 1.38$ Å) involved in the formation of bonds, which indicates that the Ge−Te (and Sb−Te) bonds in the crystalline phase are not purely covalent [33].

Figure 10 shows the Fourier transformed EXAFS spectra measured at the K-absorption edges of germanium, antimony, and tellurium, which are somewhat analogous to the radial distribution function. From the Fourier transforms of the EXAFS spectra of the crystalline phase, it can be seen that in the spectrum measured at the Te K-edge, the second coordination peak is clearly expressed, corresponding to the second-nearest Te−Te distances that indicate the existence of an ordered face-centered cubic (FCC) tellurium sublattice. At the same time, there is only one peak in the germanium spectrum. This situation is typical for disordered materials and indicates that the germanium sublattice is disordered. In other words, the structure of the material can be imagined as an ordered FCC lattice, in which the germanium atoms, displaced from the center, are located in a stochastic manner, by analogy with the paraelectric phase of the binary GeTe.

The second end material, Sb_2Te_3, is a van der Waals crystal and has a layered structure in which quintuple layers with a sequence of layers Te-Sb-Te-Sb-Te are interconnected

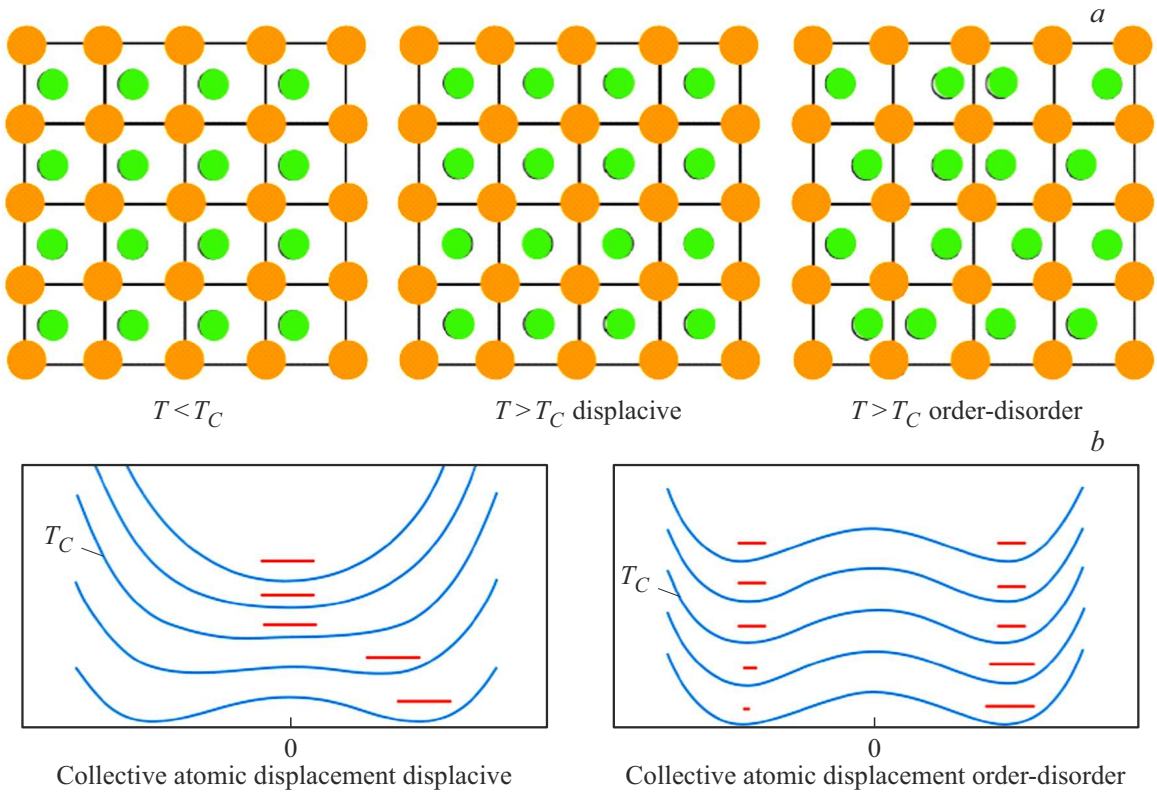

Figure 9. Schematic representation of a displacive (a) and order-disorder (b) transitions, illustrated using a configurational diagram.

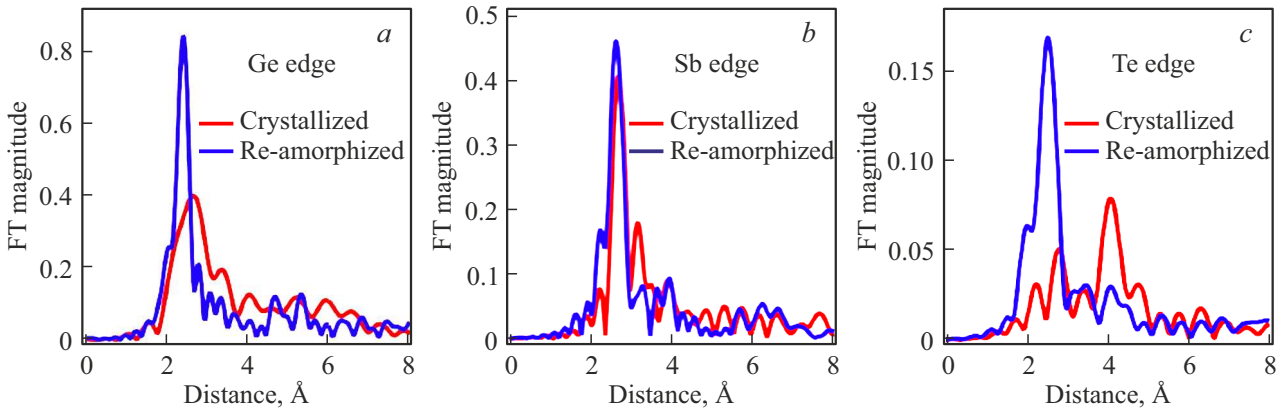

Figure 10. Fourier transforms of EXAFS spectra measured at Ge, Sb, and Te *K*-edges for crystalline and amorphous (reamorphosed) $Ge_2Sb_2Te_5$ films [33].

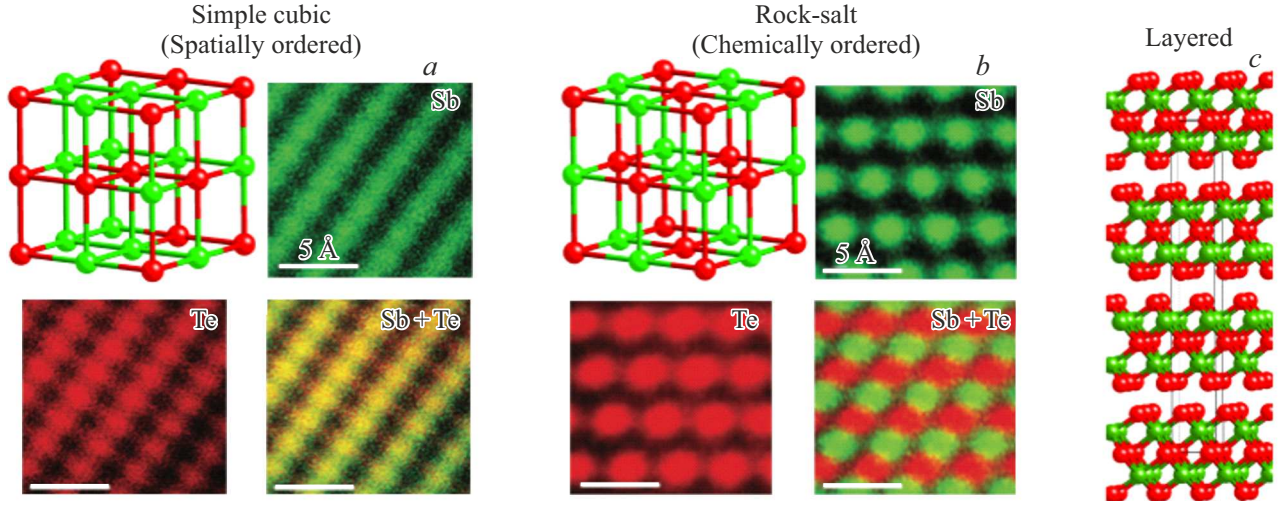

Figure 11. Metastable simple cubic (*a*) and chemically ordered (*b*) lattices Sb_2Te_3 [37]; stable layered phase Sb_2Te_3 (*c*).

by weak van der Waals bonds (Figure 11, *c*). It should be noted that this material is a classic topological insulator [34] and, like GeTe, one of the best thermoelectrics [35].

In the case of solid-state crystallization of Sb_2Te_3, a simple cubic lattice with stochastic filling of sites with antimony and tellurium atoms is first formed from the amorphous phase (Figure 11, *a*), from which later as a result of chemical ordering a rock-salt structure is formed (Figure 11, *b*) [36,37]. At the same time, since the number of cations and anions is different, cationic vacancies are formed in the material, which are randomly distributed in space. With a further increase in temperature, vacancies become ordered, resulting in the formation of a layered crystal.

2.2. Amorphous phase

Studies of the structure of the amorphous phase turned out to be more complex and ambiguous. Thus, the Ge atoms in most compounds are sp^3-hybridized and, accordingly, tetrahedrally coordinated, while the usual coordination of chalcogen atoms is equal to two, a classic example of which are $GeSe_2$ crystals. It is logical to expect that germanium and tellurium atoms in the amorphous phase will fulfill these valence requirements. However, experimental data on this subject are contradictory: the coordination numbers were determined as Ge(4):Te(2) in Ref. [38,39] by X-ray diffraction analysis and Raman spectroscopy, while experiments on EXAFS and neutron scattering in Refs. [40,41] indicate the coordination number Ge(3).

In earlier works, it was assumed that during the amorphization process, the long-range crystalline order disappears while maintaining the short-range order. Experimental studies using EXAFS [33] have shown that the situation is much more complicated. It should be noted that in the cited work the amorphous phase obtained reversibly by laser exposure, as in the case of switching in an optical disk, was used.

When comparing the spectra obtained for the crystalline and amorphous states, several features of the spectrum

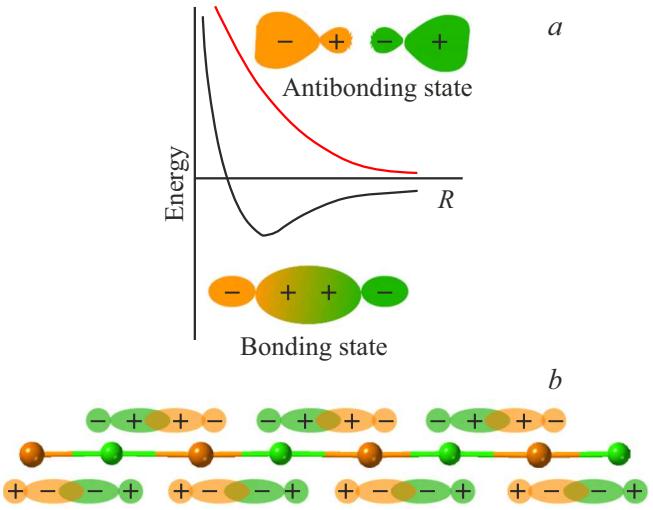

Figure 12. Schematic formation of a covalent bond due to *p*-orbitals (*a*) and variants of pairwise bonding of Ge and Te atoms in the rock-salt structure (*b*).

obtained at the Ge *K*-edge are unusual from the first glance. Firstly, the spectrum is much more intense and narrower for the amorphous phase, which is extremely unusual, since amorphization should lead to a wider distribution of interatomic distances. Secondly, the peak corresponding to the first coordination sphere is shifted in the amorphous phase towards smaller distances, which is also unusual. As a rule, due to the anharmonicity of interatomic potentials, amorphization is accompanied by an increase in bond lengths.

It clearly follows already from the visual examination of the EXAFS spectra that the process of GST amorphization is not just a loss of long-range order, but significant changes occur in the short-range order. It should be noted that in the amorphous phase, the lengths of the Ge–Te (2.61 Å) and Sb–Te (2.85 Å) bonds are almost equal to the sum of the covalent radii [33]. In other words, the amorphous phase is a covalent glass. Based on the analysis of the XANES (*X*-ray absorption near-edge spectra) spectra of the crystalline and amorphous phases, the authors suggested that germanium atoms in the amorphous phase were tetrahedrally coordinated.

The unusual nature of chemical bonds in a crystalline GeTe was first discussed in Ref. [42]. The valence electrons of Ge and Te atoms are sufficient to form three covalent bonds. At the same time, in the rock-salt structure, each atom has six such bonds. This contradiction can be understood by considering the mechanism of covalent bond formation due to *p*-orbitals (Figure 12, *a*). Depending on the symmetry of the wave functions, schematically indicated in the figure by the symbols „+“ and „–“, bonding or anti-bonding states are formed. It can be assumed that covalent bonds are formed between *pairs* of atoms (Figure 12, *b*). At the same time, the symmetry of the wave functions between such pairs (between the back-lobes of the *p*-orbitals) in the rock-salt structure also turns out to be the same, which means that covalent bonds can form between alternative pairs of atoms. Since the energies of these two configurations are the same, a resonance between them is possible.

This idea was developed in Ref. [43] and became known to most researchers thanks to this particular article. Later, the authors proposed the term „metavalent bond“ to describe the bonds in GeTe and related materials [44]. It should be noted here that the concept of metavalent bonds, although widely used, has not become generally accepted. So, in a recent article titled „The myth of ‘metavalency’ in phase-change materials“, which speaks for itself [45], it is argued that the interatomic bond existing in GST is not new but rather it is a hypervalent bond known to chemists for a long time. To avoid ambiguities related to terminology, we will call the short (strong) bonds formed with the participation of *p*-orbitals primary bonds, and the long (weak) bonds due to the interaction of back-lobes of *p*-orbitals will be called secondary bonds.

The existence of energy hierarchy of bonds is a fundamental characteristic of phase-change materials, and it is this feature that enables their functioning. It was shown in Ref. [46] that it is the breaking of secondary bonds during structural distortions caused by atomic displacements as a result of system excitation that leads to amorphization (loss of long-range order) (Figure 13). As can be seen from the figure, in the case of undirectional ionic bonds, the distorted structure of NaCl, for example, due to exposure to a pulse of light or current, reverts to the ideal structure. At the same time, a similarly distorted GeTe crystal lattice falls apart with a loss of long-range order after the excitation is removed. In the same paper, it was shown that it is the breaking of secondary bonds, rather than the subsequent disordering of the structure, that is responsible for the contrast of optical properties between the two phases (Figure 14).

As for the structure of the amorphous phase, the impetus for its active research was the pioneering work in Ref. [33], which demonstrated a significant short-range difference between the crystalline and amorphous phases and suggested that Ge atoms in the amorphous phase are tetrahedrally coordinated. In a series of papers by different authors, calculations using density functional theory have shown that in the amorphous phase, a fraction of germanium atoms are tetrahedrally coordinated (in different papers from 30 % [47,48] to 65 % [49]), which is in agreement with the conclusion made in Ref. [33]. At the same time, the remaining part of germanium atoms retains a local structure close to that in the crystalline phase, namely, they have from 3 to 6 neighbors and valence angles close to 90° (Figure 15). *In silico* crystallization studies have led to the conclusion that this process consists in the ordering of ABAB blocks (A = Ge, Sb; B = Te), resembling the structure of the crystalline phase [47,50] (Figure 16).

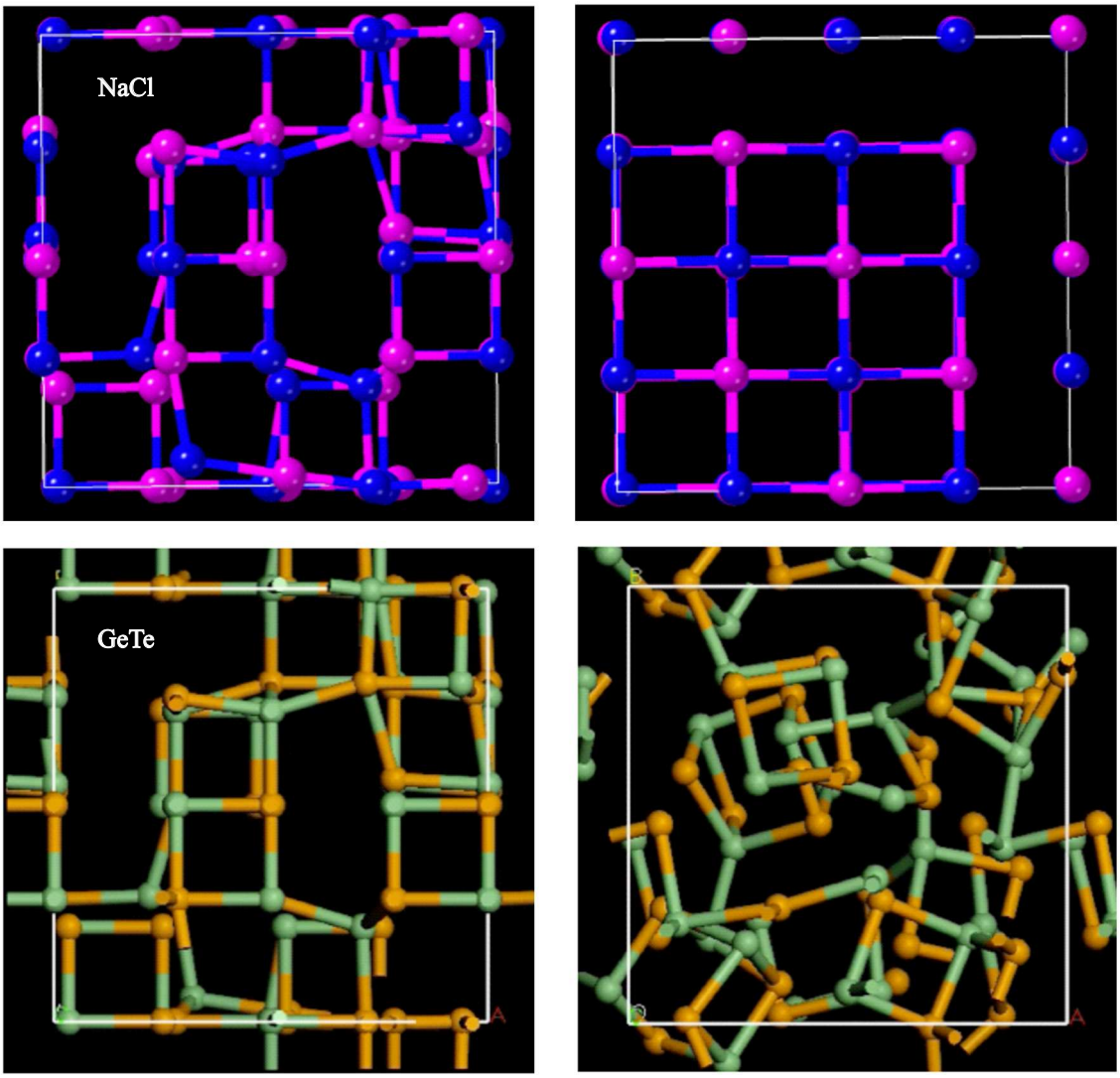

Figure 13. The structure of NaCl (upper panels) and GeTe (lower panels), distorted due to excitation (left) and relaxed after removal of excitation (right).

An interesting property of the amorphous phase is the gradual increase in its resistance over time (Figure 17) [51–53], although — if we assume that this is due to the initial stage of the crystallization process — we should expect a decrease in resistance. This phenomenon, harmful from the point of view of practical application, associated with structural relaxation and called drift, will be discussed in more detail in one of the following sections.

The AIST alloy used in +/−RW optical disks has the A7 structure (Figure 18) [54], analogous to the structure of bismuth. It is interesting to note that, just as in the GeTe and GST structures, there are also short and long bonds in the AIST structure. As a mechanism of phase transformation in AIST, the order-disorder process was proposed, similar to the process of formation of the paraelectric phase GeTe from the ferroelectric phase (Figure 19), when structural fragments formed by long and short bonds change from the ordered state to the disordered state [54].

2.3. Contribution of electronic excitation to the amorphization process

We now consider the role of electronic excitation in the amorphization process. Despite the fact that the generally accepted consensus is that the amorphization of the structure is due to its melting as a result of heating during optical excitation or the release of Joule heat when exposed to current pulses, this approach should be treated with caution. Indeed, if the energy of an optical pulse is so high that nonradiative recombination of unequal carriers, accompanied by an increase in temperature, leads to melting of the material, then a sufficiently high concentration of non-equilibrium charge carriers is generated during the excitation process, the presence of which should affect the interatomic interaction by analogy with the well-known phenomenon of optical melting of semiconductors [55,56]. There are both theoretical and experimental studies con-

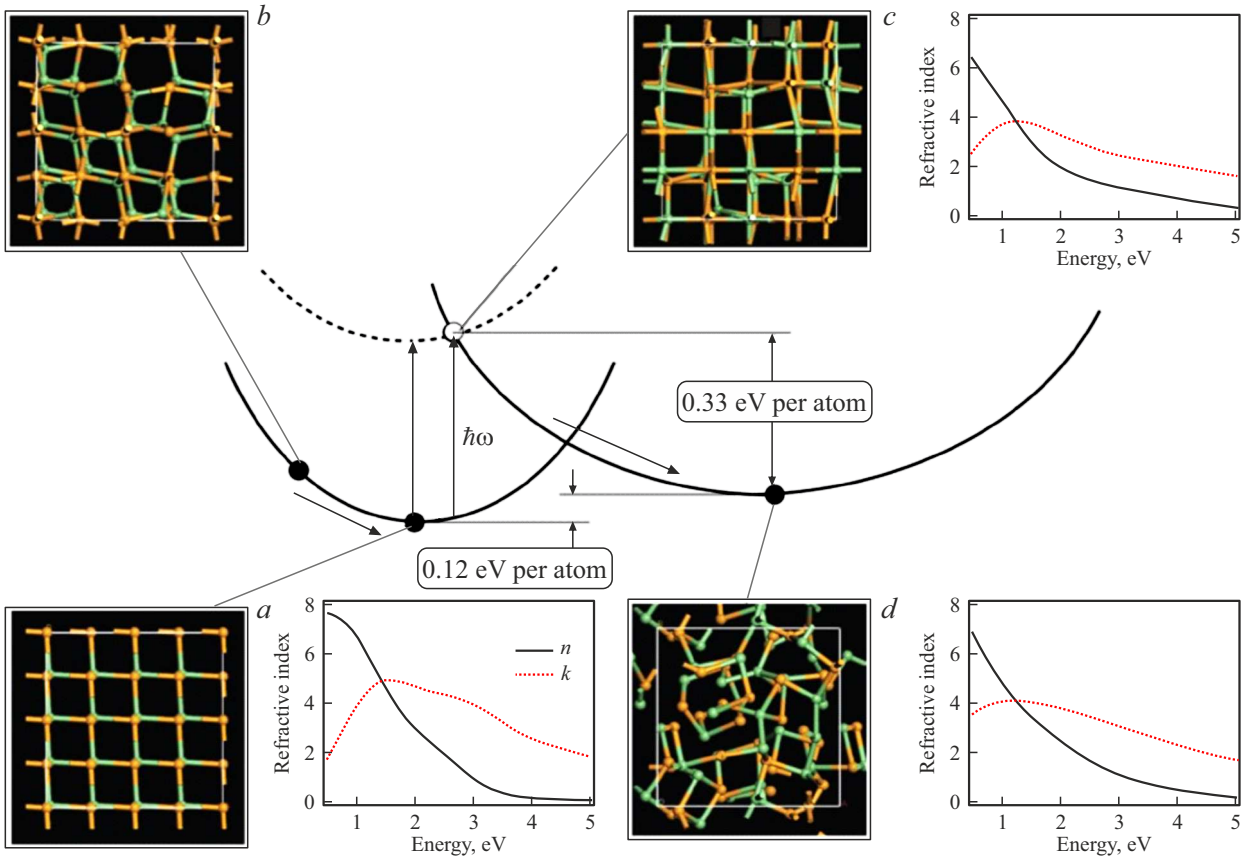

Figure 14. The nature of the optical contrast between the crystalline and amorphous phases of GeTe. It can be seen that the optical properties change immediately after the disappearance of the secondary bonds. Subsequent disordering of the structure does not lead to noticeable changes in the optical parameters [46].

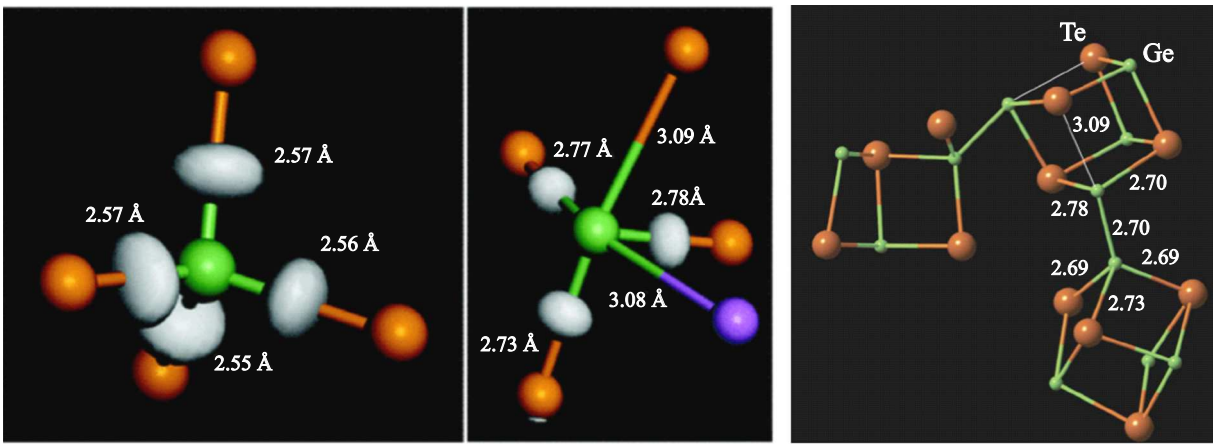

Figure 15. Local structure of Ge atoms in the amorphous phase: *a* — a tetrahedral fragment; *b* —a defective octahedral fragment; *c* — The formation of Ge–Ge bonds.

firming the important role of electronic excitation in the amorphization process.

This was for the first time demonstrated in Ref. [57]. Using calculations based on constrained DFT, the authors showed that after excitation of 9% of the valence band electrons, which is close to the concentration of excited electrons when exposed to femtosecond pulses in related experiments, the crystal structure falls apart, transforming into amorphous at temperatures significantly lower than the temperature of conventional melting (Figure 20). Moreover, it was demonstrated that the radial distribution function at different stages of the amorphization process differs signifi-

cantly from that for the thermally molten phase. (Figure 21). It also turned out that the diffusion lengths of atoms in the melt are significantly longer than during amorphization in the excited state. The results obtained clearly indicate that electronic excitation (at least at high excitation densities in the case of pico- and femtosecond pulses) plays, if not a decisive, then a very significant role. Similar results were later obtained for other phase-change materials [58,59].

The calculated results described above are in good agreement with the experiment. The amorphization process under picosecond pulse excitation was studied in Ref. [60] by the pump-probe method using X-ray absorption spectroscopy (XANES — *X*-ray absorption near-edge spectra). The authors used the fact that the XANES spectra of GST are weakly dependent on temperature (with a constant structure) and at the same time differ significantly from

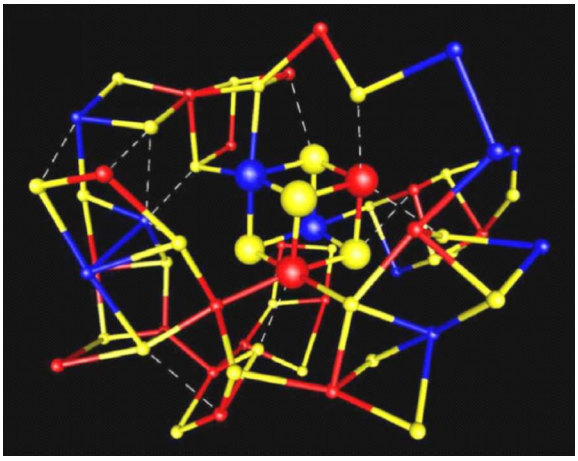

Figure 16. Cubic fragments in the amorphous phase [47].

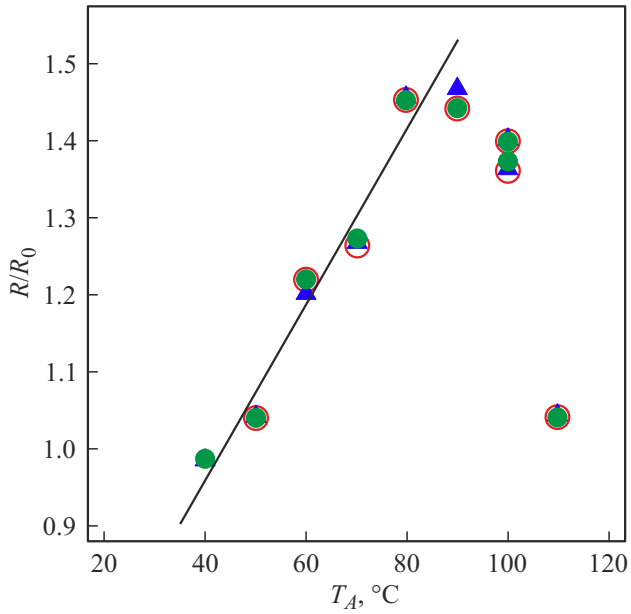

Figure 17. Conduction drift in the amorphous phase [52].

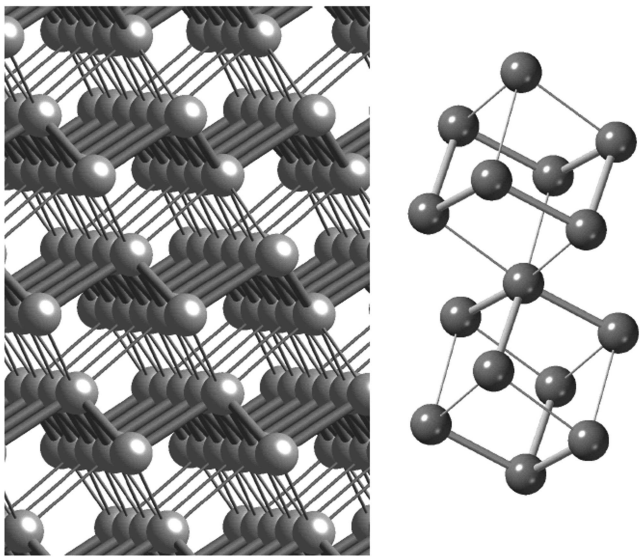

Figure 18. Crystal structure (*A*7) of the phase-change Ag–In–Sb–Te (*a*). Within the framework of this structure, cubic fragments (*b*) with short and long connections, depicted as thick and thin lines, can be distinguished.

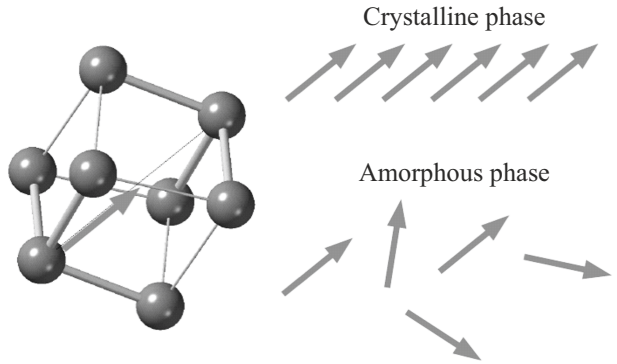

Figure 19. Schematic representation of the AIST amorphization process.

each other for crystalline, amorphous and liquid states, primarily in the intensity of the first peak, called white line (Figure 22, *a, b*). In the experiment, the phase-change material was studied in the structure of an optical disk and alternately amorphized and recrystallized by laser pulses. An X-ray pulse probed the area of the laser exposure after a certain delay time.

The experimental results shown in Figure 22, *c* demonstrate that after irradiation with a laser pulse, the intensity of the white line decreases from the value corresponding to the crystalline state to the value corresponding to the amorphous state. At the same time, the value of the white line does not reach the value corresponding to the liquid phase, which fully confirms the results of ab-initio calculations and demonstrates the important role of electronic excitation in the process of amorphization by short pulses.

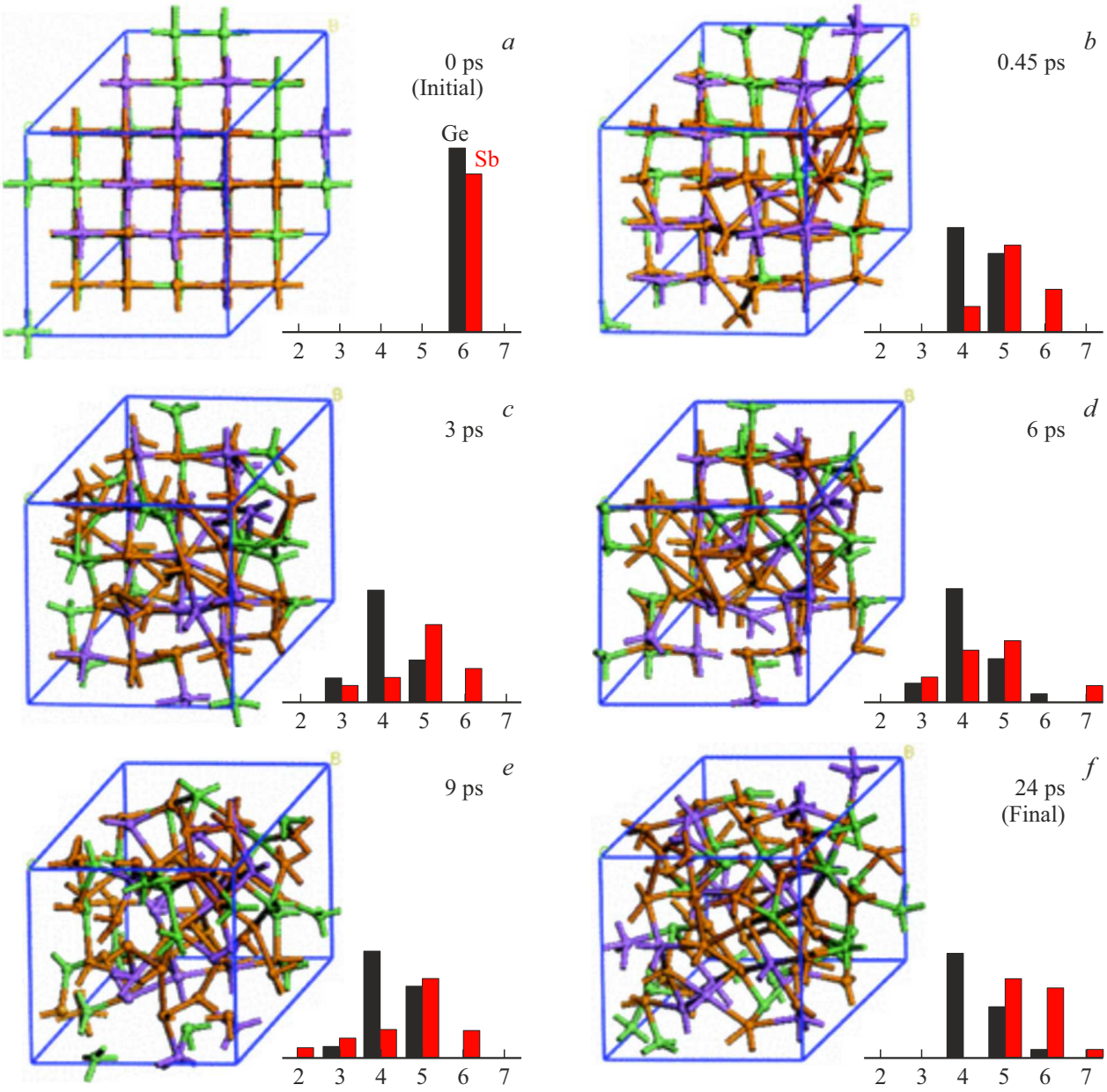

Figure 20. Evolution (amorphization) of the $Ge_2Sb_2Te_5$ structure in the excited state [57].

3. Commercial memory elements based on phase-change materials

The first surge of commercial interest in phase-change materials was observed in the early 1970s in connection with the advent and rapid spread of computers in general and personal computers in particular. Energy Conversion Devices, established by Stanford Ovshinsky and Intel jointly developed the first electrical memory cell (256 bits) based on phase-change materials in 1970. The cell consisted of a memory element connected in series with a silicon diode. Due to various technical problems, this product did not enter the market, but interest in phase-change memory continued to grow and several leading manufacturers acquired licenses for its development and production. Among them were Intel (2000), ST Microelectronics (2003), Samsung (2003), Elpida (2005), Qimonda (2007) and others. The first commercial product was BAE Systems' phase-change chips (July 2006), and in September of the same year Samsung announced the production of PRAM (512 Mbit) [61]. However, until recently, the niche occupied by phase-change non-volatile memory remained very small.

The situation was much more successful with optical memory. An optical disk was implemented in 1989 that allowed for more than 1,000,000 information rewriting cycles [62]. A year later, Matsushita introduced its first commercial product, which launched a series of rewritable

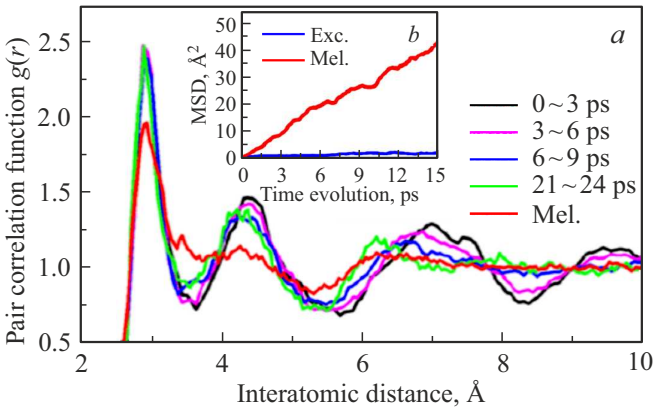

Figure 21. *a* — evolution of the correlation function $Ge_2Sb_2Te_5$ in the excited state compared to that for the melt (Mel.); *b* atomic displacements of atoms during amorphization in the excited state (Exc.) and melt (Mel.) [57].

optical discs. Rewritable DVD-RAM discs were introduced in the market in 1998 and had a capacity of 2.6 GB (version 1), in 2000 Panasonic introduced DVD-RAM with a capacity of 4.7 GB (version 2), and it is usually assumed that the capacity of DVDs is exactly 4.7 GB. A photograph of one of the first optical discs and the corresponding reader/recorder is shown in Figure 23.

The principle of operation of a rewritable optical disc is shown in Figure 24. The upper panel shows a sequence of rewriting pulses superimposed on a „pedestal" of the erasing light exposure. With this method, any previously recorded information is erased and new information is written on top of it, as illustrated in the middle panel. After that, when reading by low-intensity light, the newly written information is retrieved.

It should be noted that the contrast of optical properties and conditions of sufficient heat dissipation are in part achieved due to the disk structure, in which, along with the phase-change material, there are additional layers, in particular a metal layer (usually aluminum), which provides both good heat dissipation and enhances optical contrast, as well as a protective layer that protects the disk from mechanical damage during operation. (Figure 25).

The quasi-binary compositions of $GeTe-Sb_2Te_3$ proposed by Matsushita/Panasonic have proven themselves to be the best phase-change material. As a rule, these materials are used in +/−RAM disks, while rewritable +/−RW discs use the alloy Ag−In−Sb−Te, based on antimony-rich Sb−Te compounds with small additions of silver and indium.

The most commonly used material is the $Ge_2Sb_2Te_5$ compound (Figure 26). It was with the use of this material that the first DVD-RAM discs were released. A composition shifted towards GeTe, namely $Ge_8Sb_2Te_{11}$ (GST8-2-11) is the working material in the next generation of optical discs (Blu-ray disc, BD). The choice of the material in this case is determined solely by its higher optical contrast in the blue laser energy range compared to GST225, which has optimal optical contrast in the infrared (CD) and red (DVD) radiation ranges [63,64].

The structure of optical disks of different generations did not change in principle, only the thicknesses of the substrate and auxiliary dielectric layers changed, as well as the parameters of the elements of the optical recording system, in particular the numerical aperture of the lenses (see Figure 27 and the table). The development of optical discs was aimed at increasing their capacity, which was achieved in various ways: by reducing the wavelength of the laser used (infrared in CD-ROMs and blue in Blu-ray), complicating the disc structure with the addition of an additional phase-change layer, using new recording

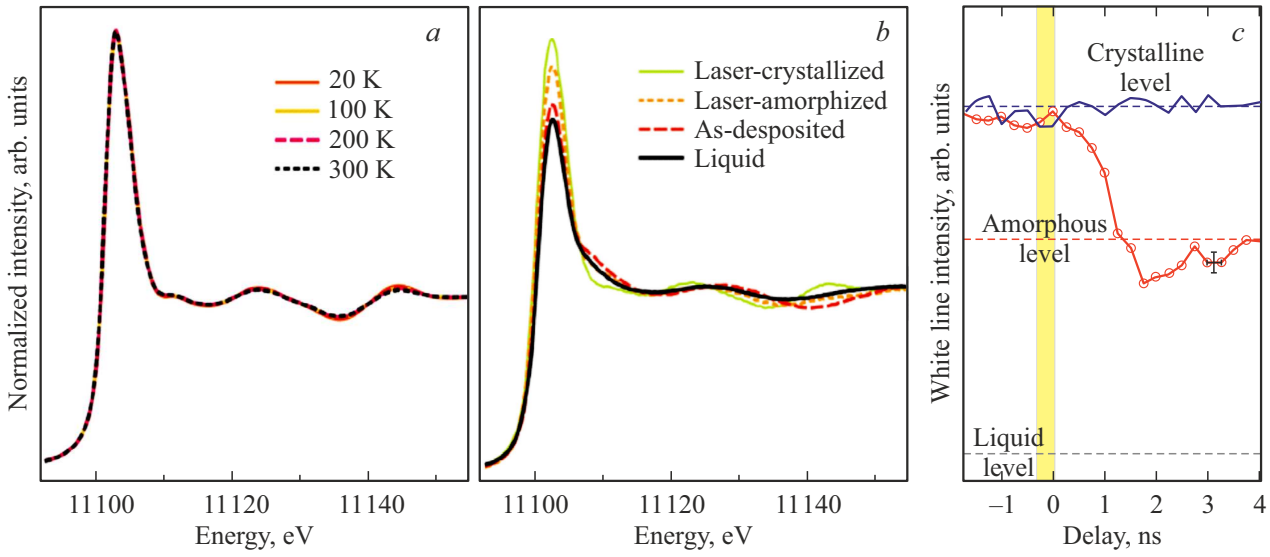

Figure 22. XANES spectra at the K-edge of Ge phase-change GST at different temperatures (*a*) and in different structural states (*b*). Kinetics of the intensity change of the „white line" during excitation by a picosecond pulse (*c*) [60].

Figure 23. Photograph of the first optical disk based on phase-change materials and the corresponding receiving device (courtesy of N. Yamada).

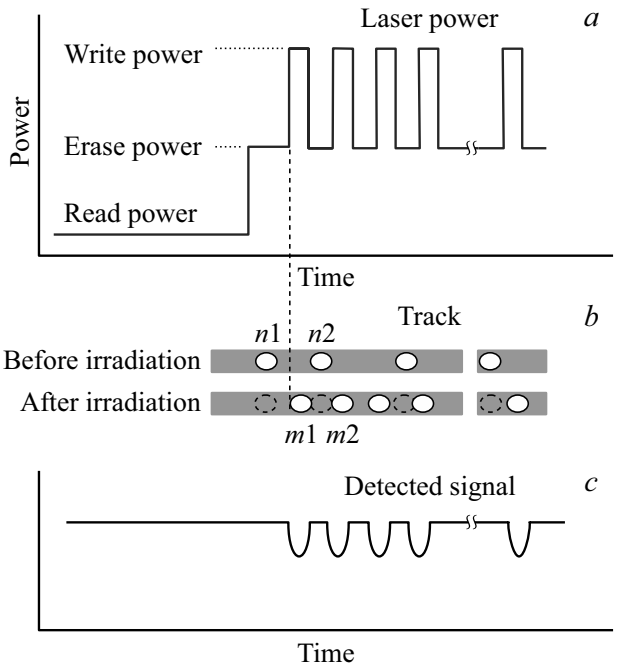

Figure 24. The principle of operation of a rewritable optical disc. During the recording process, the disc is constantly irradiated with „crystallizing" radiation, erasing previously recorded information, more powerful pulses lead to the formation of overwritten amorphous regions: *a* — pulse shape; *b* — marks on the track before and after rewriting; *c* — detected signal.

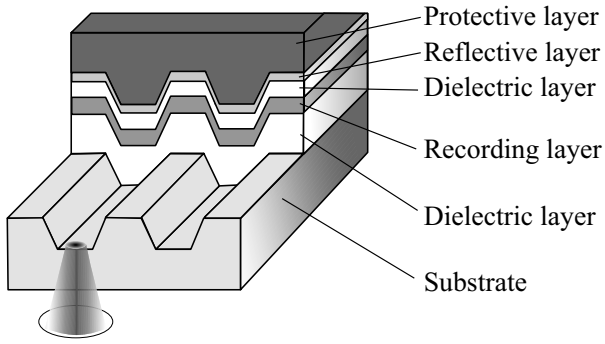

Figure 25. The layered structure of an optical disc.

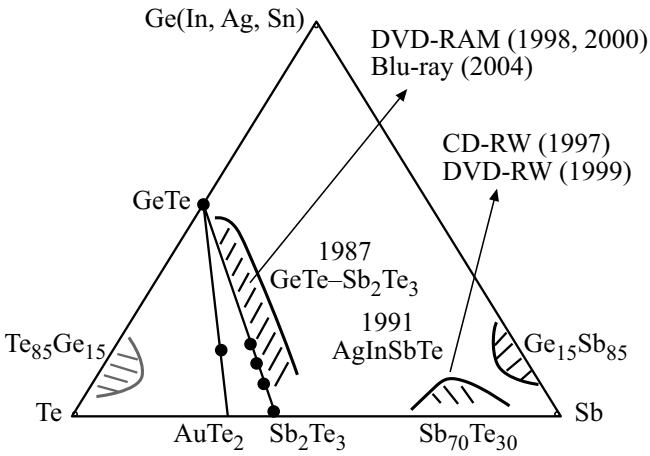

Figure 26. Materials used in optical discs.

principles, in particular using optical near field (Super-RENS [65] disks).

As for non-volatile memory, the breakthrough was the joint product of Intel and Micron 3D XPoint, which entered the market in 2015 under the commercial name Optane® [66]. The appearance of this product has to some extent revolutionized the information storage industry, which has been dominated by Flash memory for about 30 years.

The structure of 3D XPoint memory is relatively simple (Figure 28). Two-layer pairs consisting of a memory cell and a selector are located at the intersection of perpendicular rows of word-line and bit-line connectors. Different from earlier generations pf phase-change memory, each cell does not have a relatively complex (and expensive) transistor attached to it. Instead, a selector is used that works on the principle of the Ovshinsky switching effect.

What is the selector is for and does it work? To answer this question, consider a fragment of a similar cell without a selector (Figure 29, *a*). Obviously, when a voltage U is applied, sufficient to switch a cell in a high-resistance state, a voltage of $U/2$ is applied to neighboring cells, which can potentially cause them to switch arbitrarily, as well as lead to errors when reading the cell state. The presence of a selector (Figure 29, *b*) allows one to avoid this problem. When a voltage of a certain value is applied, the selector is activated and information is read or written only in the addressable selected cell.

A distinctive feature of the 3D XPoint memory is its layered structure, which makes it possible to significantly

Parameters of the optical recording system elements

Type of optical disk	Year of production	Capacity, GB	Minimum tag size, μm	Pitch, μm	Wavelength of laser, nm	Numeric lens aperture
CD	1997	0.650	0.833	1.60	780	0.50
DVD	2000	4.7	0.41	0.615	650	0.60
Blu-ray	2003	23.3	0.149	0.32	405	0.85

increase the memory capacity. The first generation of 3D XPoint had a two-layer structure and was carried out using a 20-nanometer technological process. In this configuration, the cell packing density of 3D XPoint was 10 times higher than that of NAND-type Flash memory

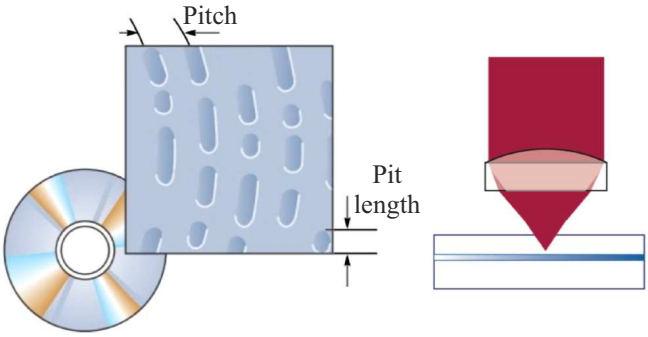

Figure 27. The scheme on an optical disc (on the left) and the information recording/reading scheme (on the right).

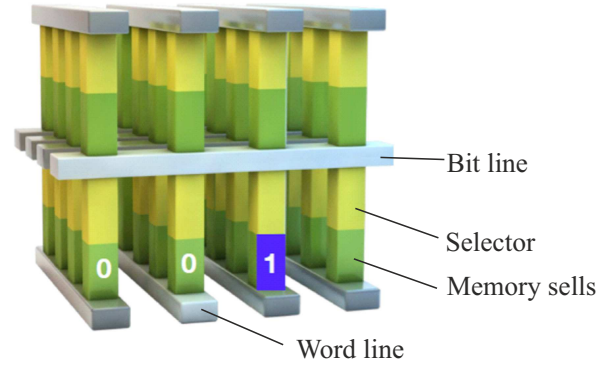

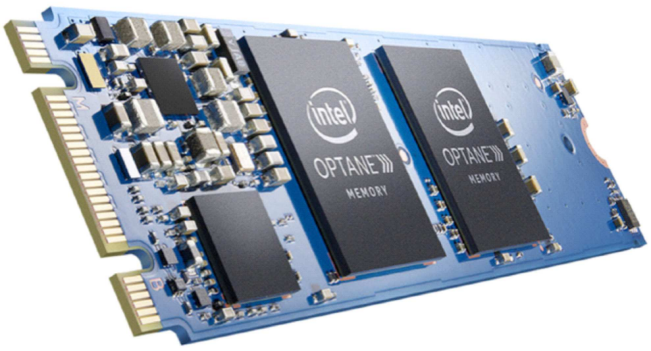

Figure 28. 3D X Point non-volatile memory structure (top) and its industrial implementation (bottom).

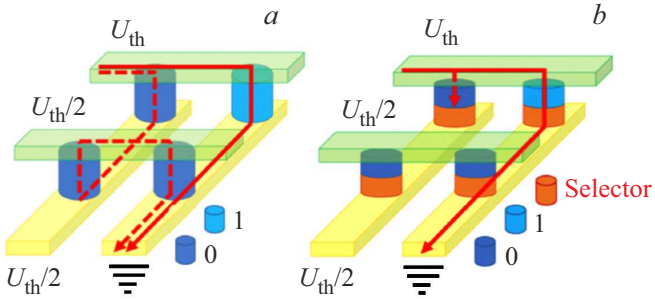

Figure 29. In a circuit without a selector, a leakage current can lead to unwanted switching of an adjacent cell or to a reading error (a). The presence of the selector ensures that only the required cell is enabled (b). The solid line in the diagrams shows the operating current. Dashed line shows the leakage current.

cells. One more fundamental difference between FLASH and 3D XPoint memory should be moted. Unlike NAND, each cell of the 3D XPoint can be accessed directly, which saves energy and does not require the use of a controller. Also an advantage of 3D XPoint memory is its greater service time. If NAND allows up to 10^3 rewrite cycles, then in the case of 3D XPoint this number increases to 10^7. At the same time, the speed of 3D XPoint is 2–3 orders of magnitude higher than that of NAND.

Once again, we emphasize that 3D XPoint memory is a Random Access Memory (RAM) type memory, i.e. it allows direct access to one memory location (one bit of information) without affecting others. Furthermore, no preparation is required before recording new information. In contrast, in NAND-type Flash memory devices, information is erased block by block, and new information is written page by page. This means that in the case of FLASH, if it becomes necessary to rewrite just one bit of information, then the entire page or all pages of the block must be overwritten, which inevitably leads to lower performance, as well as increased wear of the memory cells.

At the time of the appearance of the Optane® memory, Intel representatives denied that it was a kind of phase-change memory. However, the analysis of dies released on the market in Ref. [67] showed that a phase-change material similar in composition to the classic GST225 was used as the memory material, and the selector is based on a chalcogenide glassy semiconductor of a composition very similar tos that proposed in 1968 by Ovshinsky.

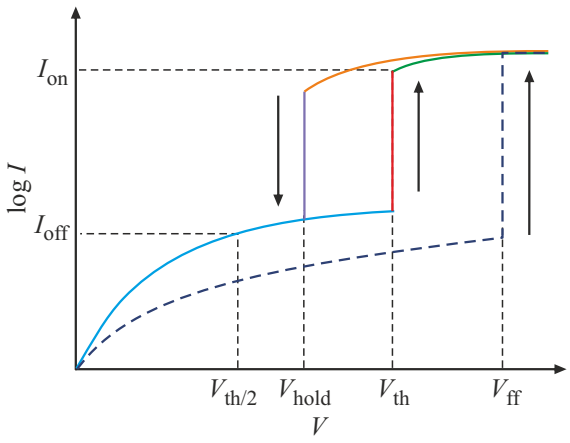

Figure 30. Schematic illustration of the Ovshinsky threshold switch (see text).

The 3D XPoint technology seemed extremely promising, but in 2022 the production of the Optane® memory was discontinued. The reasons for this decision were not reported. One of the possible reasons could be problems with the complex structure of the device. The presence of two working layers (memory and selector) in one memory element, firstly, complicates (and increases the cost of) the technological process and, secondly, can serve as an obstacle to reducing the size of the elements. In addition, there may also be difficulties with increasing the number of layers in devices. Nevertheless, encouraging news were released in 2025.

An official announcement was released in April 2025 on the website of STMicroelectronics, one of the leading European manufacturers of microelectronics, about the launch of a new memory technology called HMOG [68]. The announcement notes that this type of memory is created on the basis of phase-change materials and will begin production from the end of 2025, primarily with the aim of further integrating xMemory directly into Stellar series microcontrollers optimized specifically for the automotive market and electric vehicles. It is assumed that this solution will simplify the architecture of car control, as well as provide flexibility and scalability of the solutions being developed, since controllers with xMemory will be compatible with artificial intelligence and machine learning applications. The use of embedded devices based on non-volatile phase-change memory, in particular in the automotive industry, is due to its high stability at elevated temperatures [69]. In particular, STMicroelectronics uses Ge-rich GST compositions [70] to increase the thermal stability of memory elements.

It should be noted that STMicroelectronics has significant experience in manufacturing PCM. In the past decade, this company has been actively engaged in the development and production of PCM together with Intel. Their joint project was named Numonyx, and it was within the framework of it that the first commercial samples of electric PCM memory were created. Since then, STMicroelectronics has continued to develop PCM technology, including manufacturing microcontrollers for the aerospace industry, combining PCM and FD-SOI (fully-depleted silicon-on-insulator) technologies within the 28-nanometer technological process [71].

In addition, developers such as SK Hynix, IMEC, and IBM have published a number of articles over the past few years on the development and testing of OTS-based storage devices. Thus, despite the often mentioned decommissioning of the Optane® devices, the technology of electric phase-change memory continues to actively develop and finds its own specific market.

As noted above, the fundamental feature of the 3D XPoint memory is the use of the Ovshinsky threshold switch (OTS) rather than the transistor as a selector, which indicates that such a switch significantly exceeds the transistor in its parameters for this application. Let's now return to the question of how the OTS threshold switch functions.

The OTS selector has a sandwich structure and can be in two states: ON and OFF As shown in Figure 30, the selector cell requires a primary activation voltage (first-fire voltage, V_{ff}). After the first cycle, a significantly lower voltage, called threshold voltage (V_{th}), can turn the cell ON. Switching back to the OFF state occurs when the voltage drops below the holding voltage (V_{hold}). These voltages, $V_{ff} > V_{th} > V_{hold}$, are important parameters of the OTS switch. Other important parameters characterizing the operation of the OTS are: (1) current and current density in the open state (I_{on}, J_{on}), (2) the leakage current in the closed state (I_{off}), (3) the ratio of currents in the ON and OFF states (I_{on}/I_{off}) or selector selectivity, (4) number of switching cycles, 5) thermal stability and 6) switching speed (t_{on}/t_{off}) [72].

A purely thermal mechanism was proposed in one of the first threshold switching models [73], which consists in the fact that positive feedback operates when an increase in temperature during Joule heating leads to an increase in carrier concentration, which in turn leads to a further increase in current. However, this model could not explain the existence of a negative differential resistance region and, moreover, did not take into account the specifics of the material in any way.

An interesting model is the nucleation induced by the electric field [74], in which an increase in current was associated with an increase in temperature and the formation of subcritical nuclei in the area of the current channel. Since the size of the nuclei remains small, they collapse after voltage is removed. However, this model has also not stood the test of time.

Most researchers currently agree that the mechanism of the switching effect is electronic. This category includes the carrier injection model [75], the Poole-Frenkel effect model [76], the bipolar avalanche model [77], and the trap-assisted hydrodynamic tunneling model [78]. All of them describe the switching effect in one way or another. However, it should be noted that such a large number of

„successful“ models indicates that there is currently no real understanding of the mechanism of the switching effect.

For practical use in memory cells, the selector material must meet a number of requirements. First, it must be resistant to crystallization when a large current passes through it in the open state (I_{on}), which means that its structure must be formed by strong saturated covalent bonds. Secondly, to achieve high density, the leakage current (I_{off}) of the OTS device obtained with $V_{th}/2$ should be $< 10^{-8}$ and the selectivity (I_{on}/I_{off}) should be $\geq 10^4$. This requires materials with a large mobility gap. Thirdly, since the most frequent reading operation in practical 3D memory requires turning on/off the OTS selector, the number of operating cycles of the OTS device should be several orders of magnitude higher than that of the memory itself (usually 10^6 cycles for PCM), i.e. it should exceed 10^8 cycles. This requires the use of selector materials with high thermal stability to avoid device failure caused by involuntary crystallization, as well as to avoid phase separation during operation. Fourthly, the amorphous state of the OTS switch must withstand the temperature 400–450 °C, which is used during technological processes at the final stage of device manufacturing, for example, during deposition of layers of insulator and contact metal, i.e., the crystallization temperature of the selector material should be > 400 °C. In addition, the switching speed of the OTS device should be faster or comparable to the switching speed of the actual memory cell, i.e. < 100 ns. The main candidates meeting these requirements are compounds based on sulfur, selenium, and tellurium [72]. Their research is actively conducted in various laboratories around the world.

4. Current trends in the development of electrical memory on amorphous chalcogenides

In the course of research on the threshold switching process of chalcogenide vitreous semiconductors, a group of scientists from the Belgian IMEC center discovered an unusual and interesting from a practical point of view phenomenon . Namely, it was found that the voltage at which the selector switches from the high-resistance to the low-resistance state depends on the polarity of the pulse used during the previous switching. In other words, the selector material has its own memory. The described effect is illustrated in Figure 31. The difference between the switching threshold voltages obtained at different polarities can reach a value of 1 V.

This result was first reported in 2022 and served as a powerful impetus for the development of a new type of 3D XPoint memory without a layer of phase-change material. This type of memory is called Self-selecting memory (SSM) or Selector-only memory (SOM). The memory of the polarity of the previous switching pulse is up to several tens of minutes, but for many practical applications this is

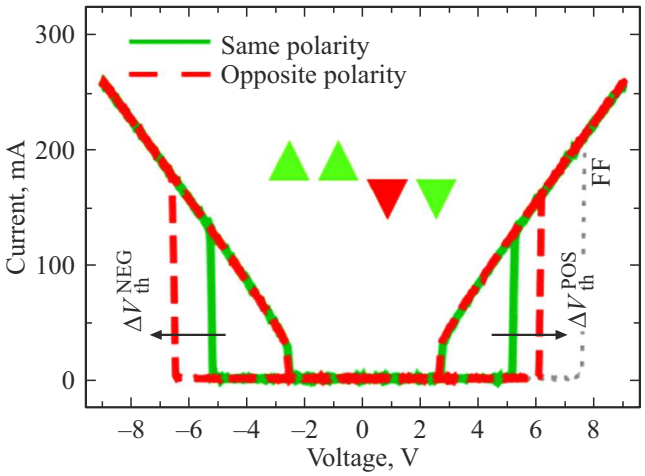

Figure 31. Switching characteristics of a threshold switch with its own memory. When switching again with a pulse of the same polarity as in the previous switching, a lower voltage is required than when using a pulse of opposite polarity.

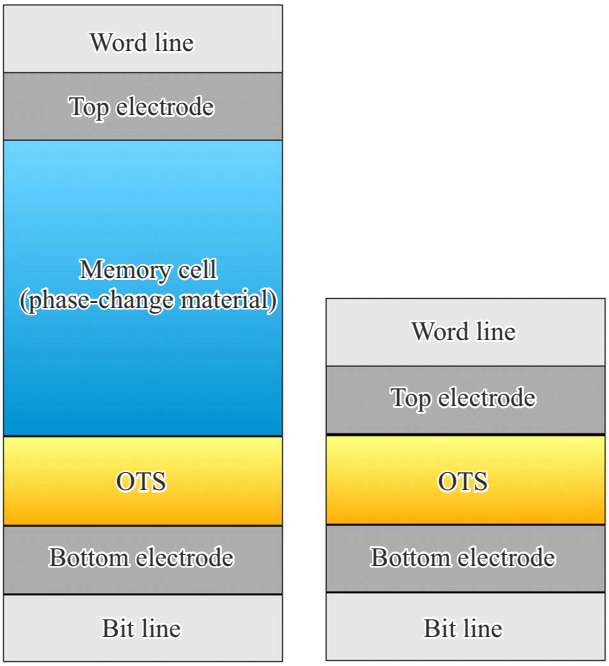

Figure 32. Structure is a non-volatile memory cell with phase-change material (on the left) and without phase-change material (on the right).

quite enough. The development of this type of memory makes it possible to significantly simplify and reduce the cost of the technological process by eliminating the phase-change material layer from the structure (Figure 32). As for the mechanism of the „selector“ memory, this question still remains open despite the active studies [79–82].

Finally, let us consider the use of phase-change chalcogenides for the development of neural networks. This area has been developing very actively in the last few years.

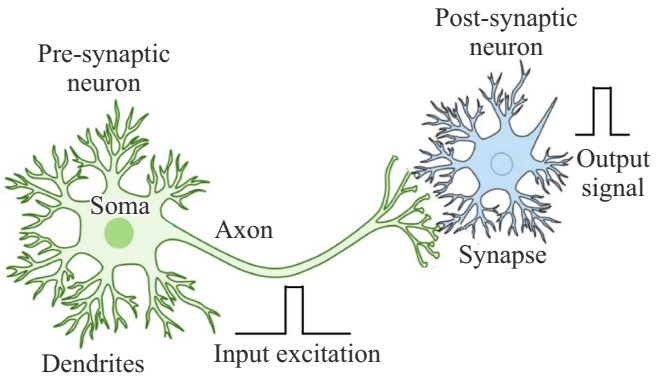

Figure 33. A fragment of the neural network of the brain (diagram).

Modern computers are based on the model proposed by John von Neumann in 1945. The so-called von Neumann architecture artificially separates data processing from storage by separating the processor and its memory. Computers based on the classical von Neumann architecture are optimal for consistently solving everyday operations. However, the continuous transfer of information in such an architecture between a storage device and a central processor, when an array of data is first transmitted to perform a calculation operation and then returned back, limits performance and energy efficiency, and, as a result, reduces the efficiency of using such systems to solve complex distributed, adaptive, and cognitive tasks. This separation of processes makes it extremely difficult to combine data obtained from multiple streams. Thus, it is becoming increasingly clear that in order to create effective cognitive computing systems, it is necessary to move to new architectures in which memory and data processing are better coordinated. Today, this is the number one unsolved problem for computing systems.

An alternative to the von Neumann architecture is cognitive or neuromorphic computers, which in turn operate according to the principle of organization and functioning of biological neural networks of a living organism, distributing processing and memory within a single system. For example, the human brain has a complex structure consisting of more than a billion neurons and trillions of synapses. Neurons consist of a soma (cell body), an axon that generates a nerve impulse, and many dendrites that receive signals from other neurons, as shown in Figure 33. A synapse is a structure that allows a neuron to transmit an electrical signal to another neuron.

Neuromorphic computing systems can be built on a similar principle and usually consist of neurons and synapses that mimic the human brain system. Each neuron is a core that processes data, and the neurons themselves are connected in parallel through synapses to transmit information. As a result, neuromorphic equipment lacks the von Neumann bottleneck limitation due to the presence of a single signal bus. However, to implement this approach in practice in the form of a hardware solution, it is necessary to develop artificial synaptic elements capable of performing the functions of biosynapses, rather than traditional devices manufactured within the framework of CMOS (Complementary Metal-Oxide-Semiconductor) technology. Figure 34 shows a comparison of the block diagram of the traditional von Neumann architecture and the neuromorphic architecture [83].

The basis of such an architecture at the moment are memristor devices, which are widely studied due to their characteristics. The term „memristor“ refers to a device combining memory and a resistor. The resistance of this device is changed by a pulse of the applied voltage and performs the function of memory for storing information for a certain period of time. Currently, work is underway to create memristors based on transition metal oxides [84], nanocomposites [85], conductive nanoparticles [86], phase-change materials [87], as well as other materials that provide a sufficiently rapid multilevel change in their state and their non-volatility. A detailed description of the main types of memristive devices and the principle of their operation can be found in the review [88].

The study in Ref. [87] was one of the first papers that demonstrated the possibility of performing calculations and constructing logic directly in the phase-change memory (in-memory computing). However, how do elements based on phase-change chalcogenide materials work for neuromorphic systems and why exactly do they appear to be one of the most promising functional materials for such calculations?

The first fundamentally important property of phase-change materials that allows performing neuromorphic calculations is their ability to form not just two levels „0“ and „1“, but a continuum of values of electrical resistance

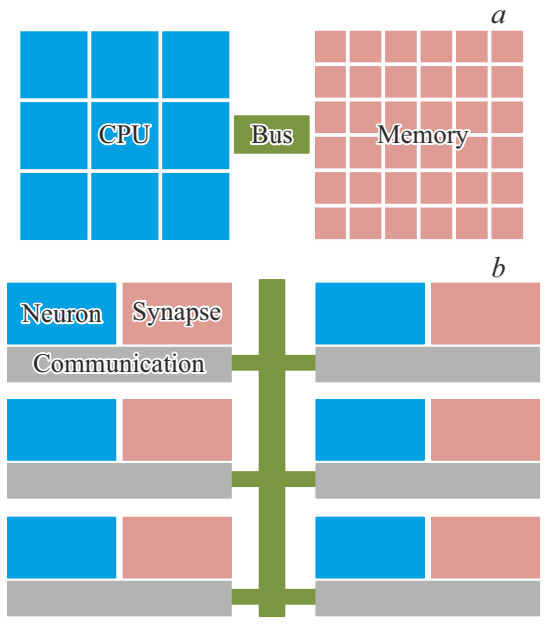

Figure 34. Block diagrams of the traditional von Neumann architecture (*a*) and a neuromorphic architecture (*b*) [83].

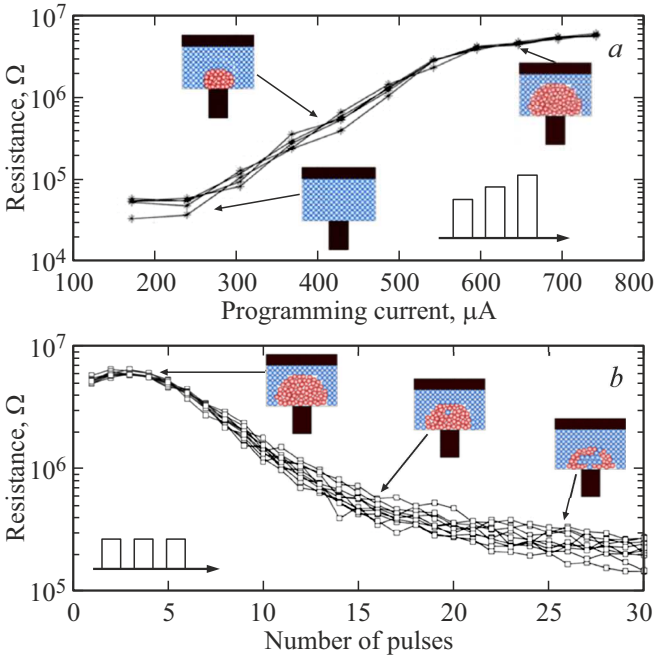

Figure 35. Programming curve (*a*) and accumulation curve (*b*), illustrating the analog recording of information [89].

(conductivity). This is usually achieved by creating intermediate phase configurations by changing the ratio of amorphous and crystalline phases. The use of appropriate electrical pulses makes it possible to partially transfer the phase-change material to the RESET state, as schematically shown in Figure 35, *a*. First, the device is programmed into a fully crystalline SET state. After that, RESET pulses of increasing intensity are applied. Figure 35, *a* shows the result of measuring the resistance of the device after each such pulse [89]. It can be seen from the figure that the resistance associated with a change in the volume of the amorphous region increases as the amplitude of the RESET pulses increases. The curve shown in the figure is called the programming curve. Thus, it is possible to ensure the formation of a state with any required resistance within the operating range of the material. In this case, it is possible to realize both an increase and a decrease in the resistance value, i. e., the programming curve is bidirectional.

The second fundamental property of phase-change materials is the cumulative crystallization process. As shown in Figure 35, *b*, the sequential application of SET pulses with the same amplitude allows for a gradual decrease in the size of the amorphous region and, consequently, the resistance of the device [89]. However, it is impossible to achieve a gradual increase in the size of the amorphous region in this way. Therefore, the curve shown in Figure 35, *b* and called the accumulation curve is unidirectional.

Currently, phase-change materials are considered one of the most suitable platforms for neuromorphic computing, as they combine: the possibility of using the properties described above to change weights in neuromorphic systems; sufficiently high switching speed and reproducibility; proven compatibility with CMOS technology, which is confirmed, among other things, by the creation of commercial non-volatile storage devices. It is precisely the high level of maturity of the technology for creating electrical storage devices based on phase-change materials that distinguishes them from the alternatives that continue to be „promising“Àt the same time, it should be noted that phase-change materials also have a number of features and issues that ask for further scientific research in this direction.

One of the key problems of phase-change materials is the drift of functional parameters.

Prototypes of tunable devices, currently being created on the basis of one of the most widely used chalcogenide materials such as $Ge_2Sb_2Te_5$, demonstrate spontaneous changes in the functional parameters of metastable states, including those manifested as a gradual increase in resistivity [90]. This phenomenon is called resistance drift. This property of the amorphous phase, mentioned earlier, needs to be minimized for the implementation of practical devices, since the drift of functional characteristics can lead to overlapping of neighboring levels and errors in reading the recorded state, which greatly complicates the implementation of multi-level cells and non-volatile elements with a continuum of levels [91].

The drift of physical characteristics in $Ge_2Sb_2Te_5$ is primarily associated with a change in the band gap and a redistribution of the density of energy states inside the gap over time [90], which, as a result, leads to a shift in the position of the Fermi level and a change in the electrophysical characteristics [92]. In a number of papers, this phenomenon is explained by changes in the defect states [93,94], relaxation of mechanical stresses [95,96], and local structural changes due to structural relaxation processes [97] and etc. However, there is still no consensus on the specific causes leading to changes in the energy and functional physical characteristics of thin films $Ge_2Sb_2Te_5$ in metastable states and research in this direction contunues For example, the evolution of the GeTe structure during drift was studied in Ref. [53] by EXAFS and it was shown that an increase in resistance correlates with an increase in the concentration of Ge−Ge bonds, which the authors attribute to an increase in the concentration of tetrahedrally coordinated germanium atoms. Concurrently with the resistance increases, the switching voltage also increases.

Currently, various approaches are being used to increase the stability of tunable phase-change elements, such as: (1) the use of complex algorithms for reading information that take into account experimentally determined drift parameters, which reduces the contrast between states and significantly increases the duration of signal processing, (2) the use of various design solutions in the cell structure, which often affects the scalability of elements, (3) the search and development of new compositions of phase-change materials in which the manifestation of the drift effect would be minimal. For example, according to the recently published results [98], a promising material for use in

neuromorphic systems may be the phase-chang composition $CrTe_3$, which practically does not demonstrate resistance drift in the temperature range from −200 to 165 °C.

5. Reconfigurable photonics and integrated optics devices for information storage and processing

The development of computing systems, including the creation of artificial neural networks based on digital or analog information processing, has demonstrated a wide range of possibilities for their effective application in various areas of everyday life. However, electronic solutions currently being developed for computing systems based on nano- and microelectronic elements are not capable of providing faster performance in the long term due to the limited bandwidth of electronic information transmission and processing speeds, including due to the influence of RC circuits (delays), as well as significant heat dissipation during the implementation of logical operations.

A promising direction for the development of hardware implementation of neuromorphic systems is the transition to fully optical elements in integrated design. Photonic integrated circuits are characterized by high throughput, noise insensitivity, high switching speed, low heat generation, and the absence of the need to apply maximum technological standards at this level of development in their manufacture. At the same time, unlike optical implementations in free space, these devices operate in the optical near field not limited by the diffraction limit, which makes it possible to miniaturize waveguide-integrated cells to nanoscale. This opens up significant prospects for the use of photonic integrated circuits to create a whole class of compact devices capable of operating in the telecommunication wavelength range with high speed and reliability.

As noted earlier, in order to create neuromorphic systems, it is necessary to ensure the creation and co-integration of components that perform the functions of a neuron, axon and dendrites, and synapse. In the case of optical implementation of such systems using photonic integrated circuits, the creation of neurons can be performed on the basis of electro-optical modulators, lasers, optical amplifiers. Thin-film waveguides can perform the function of „axon and dendrite“ (information transmission). Synapse function (changing and memorizing synaptic weights) elements based on a grid of Mach-Zehnder interferometers, optical ring resonators, and optical memristors. A detailed description of these approaches is presented in Ref. [99]. However, in the framework of this review, we will limit ourselves to considering an approach based on the creation of micro-sized fully optical memory elements and memristors in the form of photonic integrated circuits capable of implementing optical computing, information processing and storage as part of the system without the use of electronic components.

Currently, the scientific community is developing various approaches and materials for creating tunable optical devices using photonic integrated circuits. There are several ways to classify the solutions being developed, but first of all, all the elements being developed can be divided into energy-dependent and non-volatile. This separation is performed from the perspective of the need to supply energy to maintain the formed states. When creating optical elements for computing systems, many researchers rely on finding the optimal ratio beteen the following parameters: speed, power consumption, scalability, reliability, and non-volatility of the recorded states. And each of these types of tunable elements has both a number of advantages and a set of disadvantages. A detailed comparison of the parameters of various energy-dependent and non-volatile tunable optical elements can be found in the review [100].

The use of phase-change materials as a programmable domain is currently one of the most developed and promising approaches in the field of creating non-volatile devices. The first prototype of non-volatile optical memory based on the integration of thin-film waveguides with phase-change materials was presented in the paper of Pernis and Bhaskaran in 2012 [101]. The principle of operation of PCM optical elements is based on phase transformations between amorphous and crystalline states, which are accompanied by a significant change in the optical properties of the material. It is important to note that such changes in the structure and properties of phase-change materials can be initiated not only by electrical but also by optical pulses, which suggests the prospects for their use in both electrical and electro-optical devices, as well as in fully optical neuromorphic systems [102–104]. The controlled phase changes, including through ultrashort laser exposure, and, as a result, changes in the refractive index and extinction coefficient of the PCM region covering the thin-film waveguide, make it possible to control the parameters of radiation propagated through the element of a photonic integrated circuit.

The principle of operation can be considered using the example of the element [105] shown in Figure 36, *a*. The element consists of two radiation input/output elements in the form of diffraction gratings connected by a linear waveguide made of silicon nitride. It should be noted that the creation of these elements is possible both on the basis of silicon nitride [106], and using other waveguide platforms: silicon-on-insulator [107], lithium niobate [108], polymers [109] and etc. A functional region of a thin film of a phase-change material is locally formed on the surface of the waveguide. In the case of an element operating in air, in order to prevent oxidation processes and create optimal heating conditions, this area is usually covered with a protective layer such as SiO_2, ITO or ZnS. After hitting the diffraction grating from free space, the laser radiation starts to propagate along the waveguide. At the moment when the radiation reaches the region with phase-change material, it is attenuated. In this case, a change in the phase state of the PCM coating leads to a change in the parameters of the optical signal passing through the waveguide (intensity and/or phase). By changing the degree of crystallization, it is possible to increase the

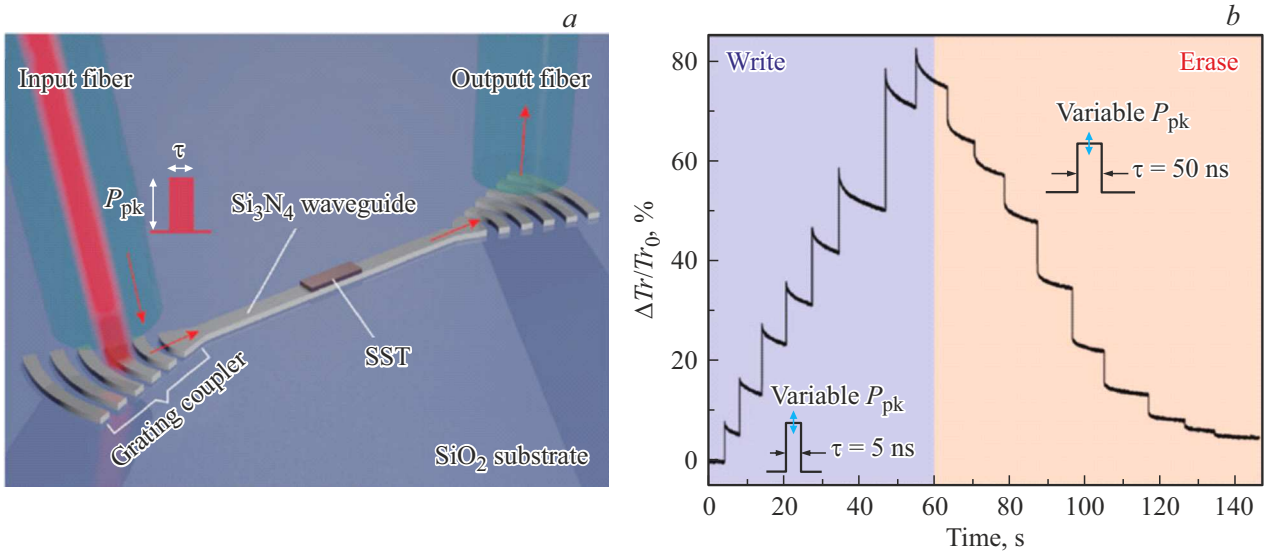

Figure 36. Integrated neuromorphic photonic memory device: *a* — schematic representation of the device; *b* — implementation of multi-level recording on $Sc_{0.2}Sb_2Te_3$ using pulses with a duration of 5 ns (for recording) and 50 ns (for erasing) [105].

effective refractive index of the waveguide mode, reaching a maximum at full crystallization, and, as a result, to provide attenuation of the signal. For example, GST in the crystalline state absorbs more light at a wavelength of 1550 nm, which leads to a stronger attenuation of the reading signal passing through the waveguide, compared with the case when GST is in an amorphous state.

In the case of creating fully optical elements, phase switching is achieved by applying a programmable pulse through the waveguide, the energy of which, partially absorbed by the functional area, will ensure heating of the material above the required temperature of the phase transition. switching can also be implemented in other ways, including by heating the phase-change material using a heating element, which can be an upper layer of ITO or doped silicon in SOI structures located under the programmable area of the PCM. Moreover, in the case of external heating, the change in transmission can be mainly due to two processes — a change in the phase state of the film of the phase-change material and a change in the optical parameters of the phase-change material, depending on the temperature [110].

A change in the phase state in such structures can occur not only quickly, but also reversibly, and maintaining the formed state of the PCM does not require energy expenditure. At the same time, fundamental studies of PCM materials show that the characteristics of the elements currently being created can be improved, in particular, the switching time of the PCM element can be < 250 ps [111], and the minimum duration and energy of the switching pulse < 1 ps [111] and 190 pJ [112] respectively. Additionally, it should be noted that an actively developing area is the search for ways to improve the parameters of the elements, including through the use of other functional materials. For example, the possibility of adjusting the switching energy and optical contrast of tunable waveguide elements is demonstrated in Ref. [113] by using an modification of $Ge_2Sb_2Te_5$ with additional elements. A detailed consideration of the modification of phase-change materials is described in Ref. [114,115]. In addition, in a large number of recent works, it is proposed to use binary compounds of antimony chalcogenides for phase memory devices, both as functional materials themselves [116] and as part of multilayer structures [117], noting that in comparison with $Ge_2Sb_2Te_5$ their optical properties are more suitable for wavelengths near 1550 nm.

The optical contrast achieved by crystalline and amorphous states is determined by both the parameters of the material itself and the geometry, including the length of the PCM region along the waveguide. It should be noted that the dependence of optical losses is not a linear function of the length of the PCM and is largely determined by the ratio of scattering and absorption contributions [118]. An interesting approach is also signal modulation due to the formation of laser-induced periodic structures on the surface of the functional region of the PCM, which can be used, for example, to ensure the spectral selectivity of the element [119]. Moreover, due to the precision variation of the parameters of the effect initiating the phase transition, it is possible to control the ratio between the volume of amorphous and crystalline fractions [120], as well as to create additional metastable states [121]. This makes it possible to create multi-level devices necessary for the implementation of an artificial synapse, the main element of neuromorphic computing systems. As an example, Figure 36, *b* shows an optical synapse implemented using phase-change material $Sc_{0.2}Sb_2Te_3$.

It should also be noted that, according to the results of broadband dielectric spectroscopy, the spectral range of possible applications of phase-change materials is much wider [122]. For example, a tunable Mach–Zender interferometer was demonstrated in Ref. [123] for O-band (1.26–1.36 μm), and a tunable attenuator operating in the sub-terahertz frequency range (126.5–145.5 GHz) was demonstrated in Ref. [124], which, together with the terahertz range, is considered promising for the development of next-generation communication systems (6G).

Since the first demonstrations of tunable integrated optical elements, the scientific community has made significant progress in this area. A number of hardware implementations of fully optical neuromorphic systems have been proposed, among which several variants can be distinguished. Thus, a photonic synapse was constructed in Ref. [125] on the basis of ring resonators locally coated with $Ge_2Sb_2Te_5$. In Ref. [126] it was proposed to use waveguide elements with sequentially applied $Ge_2Sb_2Te_5$ regions as an isolated artificial photonic synapse, which is connected to neurons at the input and output of the waveguide. Later, a similar approach was used in Ref. [127], where photonic synapses were integrated with fully optical neural circuits, also formed on the basis of $Ge_2Sb_2Te_5$. Using the proposed architecture, the authors demonstrated the possibility of creating a fully optical neuromorphic system and its learning ability. It is on the basis of phase-change materials that the possibility of creating a photonic tensor core based on phase-alternating materials was demonstrated [128].

A number of main problems faced by researchers and developers when creating optical neuromorphic computing systems should be mentioned: a low degree of miniaturization of elements; optical losses as a result of heterointegration; suboptimal operation of neurons and synapses; the need to optimize functional passive elements, including interconnects. A detailed description of the current challenges is provided in Ref. [129].

Solving these problems requires the development of additional constructive, technological and materials science solutions, for example, the search for new materials, technologies for forming and introducing them into existing production lines.

Nevertheless, the area responsible for the development of integrated photonics elements, including those based on phase-change materials, is included in a number of Roadmaps for the development of neuromorphic computing, compiled with the participation of leading research organizations [130,131], and the use of PCM materials in photonic integrated circuits is noted as one of the most promising directions. An interested reader can be refered to numerous recent reviews on this topic [132–136].

It is impossible to ignore the fact that the development of photonics and optoelectronics, associated with increased attention to the limitations of the speed of transmission and processing of information, requires, in addition to the development of reconfigurable photonic integrated circuits, the development of various methods and structures used to effectively control the transmitted optical signal and the direction of its propagation. Currently, various designs and prototypes of metasurfaces and metamaterials are being actively developed based on phase-change materials [137,138] for optical modulation of the light signal [139], controlling the shape of the light beam and the direction of its propagation [140], and controlling the absorption of optical systems [141,142]. An interesting approach is direct laser recording and erasure of two-dimensional structures, with the help of which the possibility of creating and rearranging elements for generating vortex beams as demonstrated in Ref. [143]. It should be noted that with the right choice of design and materials, crystallization in thin films of $Ge_2Sb_2Te_5$ can be achieved even using single femtosecond pulses [144]. In this case, these metasurfaces can be switched both by laser radiation and by using Joule heating [145].

Based on phase-change materials, including $Ge_2Sb_2Te_5$, the creation of a wide variety of elements has been demonstrated: prototypes of reflective displays [146], electro-optical modulators [147,148], active antennas [149,150], wave plates [151], holographic elements [152], thermal masking [153], which testifies to the incredible versatility of phase-change materials and the possibility of their application in a wide variety of fields of science and technology, far beyond the limits of memory devices and information processing systems.

6. Conclusion

In conclusion, we would like to note once again that the discovery of the semiconductor properties of chalcogenide glasses, made at the A.F. Ioffe Physical-Technical Institute in the mid-1950s, had a huge impact on the development of semiconductor physics and technology. From the point of view of physics, it was demonstrated that the existence of a long-range crystalline order is not a necessary condition for the presence of a band gap in the energy spectrum of a material, which led to a change in the previously existing paradigm. As for the practical aspect, taking into account the increasing demands for memory capacity and its performance, in particular in connection with the development of artificial intelligence and the so-called big data, it can be said with confidence that chalcogenide vitreous semiconductors have occupied and have been holding the leading positions in the memory market for many years and are one of the most promising materials for building future electronic and photonic neuromorphic computing systems .

Funding

The authors of the paper express their gratitude to the Russian Science Foundation for partial support of this work under a joint grant from the Russian National Science Foundation (grant 25-49-00103) and the National Foundation for Natural Sciences of China (NSFC).

Conflict of interest

The authors declare that they have no conflict of interest.

References

[1] B.T. Kolomiets, N.A. Goryunova. ZhTF, **25** (6), 984 (1955). (in Russian).
[2] N. Mott. Science, **201** (4359), 871 (1978).
[3] B.T. Kolomiets. J. Non-Cryst. Solids, **59**, 973 (1983).
[4] S.R. Ovshinsky. Phys. Rev. Lett., **21** (20), 1450 (1968).
[5] L. Hoddeson, P. Garrett. *The Man Who Saw Tomorrow: The Life and Inventions of Stanford R. Ovshinsky* (Cambridge, Massachusetts, USA, MIT Press, 2018).
[6] The US Congress, Minutes of the meeting of September 11, 2012 p. S6103. Available at: https://www.congress.gov/112/crec/2012/09/11/CREC-2012-09-11-pt1-PgS6103.pdf (Date of access: 01.10.2023).
[7] S. Raoux, M. Wuttig. *Phase-Change Materials: Science and Applications* (Berlin, Germany, Springer, 2009).
[8] A.V. Kolobov, J. Tominaga. *Chalcogenides: Metastability and Phase-Change Phenomena* (Heidelberg, Germany, Springer, 2012).
[9] *Elektronnye yavleniya v khal'kogenidnykh stekloobraznykh poluprovodnikakh*, pod red. K.D. Tsendin (M., Nauka, 1996). (in Russian).
[10] J. Orava, A.Á. Greer, B. Gholipour, D.W. Hewak, C.E. Smith. Nature Materials, **11**, 279 (2012).
[11] N. Yamada. MRS Bulletin, **21**, 48 (1996).
[12] N. Yamada. Rev. Laser Eng., **28** (9), 585 (2000).
[13] H. Iwasaki, Y. Ide, M. Harigaya, Y.K. Kageyama, I.F. Fujimura. Jpn. J. Appl. Phys., **31** (1), 461 (1992).
[14] R.O. Jones. J. Phys.: Condens. Matter, **37**, 113001 (2025).
[15] N. Yamada, T. Matsunaga. J. Appl. Phys., **88**, 7020 (2000).
[16] T. Nonaka, G. Ohbayashi, Y. Toriumi, Y. Mori, H. Hashimoto. Thin Sol. Films, **370**, 258 (2000).
[17] E.A. Stern, Y. Yacoby. J. Phys. Chem. Solids, **57** (10), 1449 (1996).
[18] D. Haskel, E.A. Stern, V. Polinger, F. Dogan. Phys. Rev. B, **64**, 104510 (2001).
[19] H. Cheng, H. Yao, Y. Xu, J. Jiang, Y. Yang, J. Wang, X. Li, Y. Li, J. Shao. Chem. Mater., **36** (8), 3764 (2024).
[20] A.V. Kolobov, D.J. Kim, A. Giussani, P. Fons, J. Tominaga, R. Calarco, A. Gruverman. APL Materials, **2** (6), 066103 (2014).
[21] C. Rinaldi, S. Varotto, M. Asa, J. Sławińska, J. Fujii, G. Vinai, S. Cecchi, D. Di Sante, R. Calarco, I. Vobornik, G. Panaccione. Nano Lett., **18**, 2751 (2018).
[22] D. Di Sante, P. Barone, R. Bertacco, S. Picozzi. Adv. Mater., **25**, 509 (2012).
[23] X. Zhang, Z. Bu, S. Lin, Z. Chen, W. Li, Y. Pei. Joule, **4**, 986 (2020).
[24] H. Cheng, J. Zhang, C. Lin, X. Li, F. Peng, G. Li, Y. Li. J. Phys. Chem. C, **122**, 28460 (2018).
[25] A.V. Kolobov, J. Tominaga, P. Fons, T. Uruga. Appl. Phys. Lett., **82**, 382 (2003).
[26] A.H. Edwards, A.C. Pineda, P.A. Schultz, M.G. Martin, A.P. Thompson, H.P. Hjalmarson. J. Phys.: Condens. Matter, **17**, L329 (2005).
[27] T. Chattopadhyay, J.X. Boucherle. J. Phys. C: Solid State Phys., **20**, 1431 (1987).
[28] M. Krbal, A.V. Kolobov, P. Fons, R.E. Simpson, T. Matsunaga, J. Tominaga, N. Yamada. Phys. Rev. B, **84**, 104106 (2011).
[29] P. Fons, A.V. Kolobov, M. Krbal, J. Tominaga, K.S. Andrikopoulos, S.N. Yannopoulos, G.A. Voyiatzis, T. Uruga. Phys. Rev. B, **82**, 155209 (2010).
[30] T. Matsunaga, P. Fons, A.V. Kolobov, J. Tominaga, N. Yamada. Appl. Phys. Lett., **99**, 231906 (2011).
[31] T. Egami, S.J. Billinge. *Underneath the Bragg Peaks: Structural Analysis of Complex Materials* (Oxford, UK, Elsevier, 2012).
[32] B.K. Teo. *EXAFS: Basic Principles and Data Analysis* (Berlin, Germany, Springer Verlag, 2012).
[33] A.V. Kolobov, P. Fons, A.I. Frenkel, A.L. Ankudinov, J. Tominaga, T. Uruga. Nature Materials, **3**, 703 (2004).
[34] H. Zhang, C.X. Liu, X.L. Qi, X. Dai, Z. Fang, S.C. Zhang. Nature Physics, **5**, 438 (2009).
[35] B. Xu, J. Zhang, G. Yu, S. Ma, Y. Wang, Y. Wang. J. Appl. Phys., **124**, 165106 (2018).
[36] Y. Zheng, M. Xia, Y. Cheng, F. Rao, K. Ding, W. Liu, Y. Jia, Z. Song, S. Feng. Nano Research, **9**, 3453 (2016).
[37] Y. Zheng, W. Song, Z. Song, Y. Zhang, T. Xin, C. Liu, Y. Xue, S. Song, B. Liu, X. Lin, V.G. Kuznetsov, I.I. Tupitsyn, A.V. Kolobov, Y. Cheng. Adv. Sci., **11**, 2301021 (2024).
[38] F. Betts, A. Bienenstock, S.R. Ovshinsky. J. Non-Cryst. Solids, **4**, 554 (1970).
[39] K. Hirota, K. Nagino, G. Ohbayashi. J. Appl. Phys., **82**, 65 (1997).
[40] S.J. Pickart, Y.P. Sharma, J.P. de Neufville. J. Non-Cryst. Solids, **34**, 183 (1979).
[41] P. Ma, H. Tong, T. Huang, M. Xu, N. Yu, X. Cheng, C.J. Sun, X. Miao. J. Phys. Chem. C, **121**, 1122-8 (2017).
[42] G. Lucovsky, R.M. White. Phys. Rev. B, **8**, 660 (1973).
[43] K. Shportko, S. Kremers, M. Woda, D. Lencer, J. Robertson, M. Wüttig. Nature Materials, **7**, 653 (2008).
[44] Y. Cheng, S. Wahl, M. Wüttig. Phys. Status Solidi RRL, **15**, 2000482 (2021).
[45] R.O. Jones, S.R. Elliott, R. Dronskowski. Adv. Mater., **35**, 2300836 (2023).
[46] A.V. Kolobov, M. Krbal, P. Fons, J. Tominaga, T. Uruga. Nature Chemistry, **3**, 311 (2011).
[47] J. Akola, R.O. Jones. Phys. Rev. B, **76**, 235201 (2007).
[48] S. Caravati, M. Bernasconi, T.D. Kühne, M. Krack, M. Parrinello. Appl. Phys. Lett., **91**, 171906 (2007).
[49] M. Micoulaut, A. Piarristeguy, H. Flores-Ruiz, A. Pradel. Phys. Rev. B, **96**, 184204 (2017).
[50] J. Hegedüs, S.R. Elliott. Nature Materials, **7**, 399 (2008).
[51] M. Boniardi, D. Ielmini. Appl. Phys. Lett., **98**, 242106 (2011).
[52] M. Boniardi, D. Ielmini, S. Lavizzari, A.L. Lacaita, A. Redaelli, A. Pirovano, IEEE Trans. Electron Dev., **57**, 2690 (2010).
[53] P. Noé, C. Sabbione, N. Castellani, G. Veux, G. Navarro, V. Sousa, F. Hippert, F. d'Acapito. J. Phys. D: Appl. Phys., **49**, 035305 (2015).
[54] T. Matsunaga, J. Akola, S. Kohara, T. Honma, K. Kobayashi, E. Ikenaga, R.O. Jones, N. Yamada, M. Takata, R. Kojima. Nature Materials, **10**, 129 (2011).
[55] K. Sokolowski-Tinten, J. Bialkowski, M. Boing, A. Cavalleri, D. von der Linde. Phys. Rev. B, **58**, R11805 (1998).

[56] A. Rousse, C. Rischel, S. Fourmaux, I. Uschmann, S. Sebban, G. Grillon, P. Balcou, E. Förster, J.P. Geindre, P. Audebert, J.C. Gauthier. Nature, **410**, 65 (2001).
[57] X.B. Li, X.Q. Liu, X. Liu, D. Han, Z. Zhang, X.D. Han, H.B. Sun, S.B. Zhang. Phys. Rev. Lett., **107**, 015501 (2011).
[58] S.C. Tiwari, R.K. Kalia, A. Nakano, F. Shimojo, P. Vashishta, P.S. Branicio. J. Phys. Chem. Lett., **11**, 10242 (2020).
[59] L. Yang, S.C. Tiwari, S. Fukushima, F. Shimojo, R.K. Kalia, A. Nakano, P. Vashishta, P.S. Branicio. J. Phys. Chem. Lett., **13**, 10230 (2022).
[60] P. Fons, H. Osawa, A.V. Kolobov, T. Fukaya, M. Suzuki, T. Uruga, N. Kawamura, H. Tanida, J. Tominaga. Phys. Rev. B, **82**, 041203 (2010).
[61] C.H. Lam. *History of Phase Change Memories.* In: S. Raoux, M. Wuttig (eds). *Phase Change Materials* (Boston, MA, Springer, 2009) c. 1.
[62] T. Ohta. J. Optoelectron. Adv. Mater., **3**, 609 (2001).
[63] N. Yamada. MRS Bull., **21**, 48 (1996).
[64] N. Yamada. Rev. Laser Eng., **28**, 585 (2000).
[65] T. Shima, T. Nakano, J. Kim, J. Tominaga. Jpn. J. Appl. Phys., **44**, 3631 (2005).
[66] *3D XPoint. Wikipedia, The Free Encyclopedia*. Access mode: https://en.wikipedia.org/wiki/3D_XPoint (date of access: 03.11.2025).
[67] *Intel 3D XPoint Memory Die Removed from Intel OptaneTM PCM (Phase Change Memory)*. Access mode: https://web.archive.org/web/20171201031032/ http://techinsights.com/about-techinsights/overview/blog/ intel-3D-xpoint-memory-die-removed-from-intel-optane-pcm/ (date of access: 05.11.2025).
[68] The official website of STMicroelectronics. Press Item № t4687 // newsroom.st.com. Available at: https://newsroom.st.com/media-center/press-item.html/ t4687.html (date of access: 04.11.2025).
[69] X. Li, H. Chen, C. Xie, D. Cai, S. Song, Y. Chen, D. Cai, Y. Lei, M. Zhu, Z. Song. Phys. Status Solidi RRL, **13**, 1800558 (2019).
[70] F. Arnaud, P. Zuliani, J. Reynard, A. Gandolfo, F. Disegni, P. Mattavelli, E. Gomiero, G. Samanni, C. Jahan, R. Berthelon, O. Weber, E. Richard, V. Barral, A. Villaret, S. Kohler et al. *Truly innovative 28 nm FDSOI technology for automotive micro-controller applications embedding 16 MB phase change memory* // Proc. IEEE Int. Electron Dev. Meet. (San Francisco, USA, 2018).
[71] The official website of STMicroelectronics. *Phase Change Memory (PCM)* // st.com. Available at: https://www.st.com/content/st_com/en/about/innovation-technology/PCM.html (date of access: 04.11.2025).
[72] Z. Zhao, S. Clima, D. Garbin, R. Degraeve, G. Pourtois, Z. Song, M. Zhu. Nano-Micro Lett., **16**, 81 (2024).
[73] D.M. Kroll. Phys. Rev. B, **9**, 1669 (1974).
[74] V.G. Karpov, Y.A. Kryukov, I.V. Karpov, M. Mitra. Phys. Rev. B, **78**, 052201 (2008).
[75] G.C. Vezzoli, P.J. Walsh, L.W. Doremus. J. Non-Cryst. Solids, **18**, 333 (1975).
[76] D. Ielmini. Phys. Rev. B, **78**, 035308 (2008).
[77] P. Fantini, N. Polino, A. Ghetti, D. Ielmini. Adv. Electron. Mater., **9**, 2300037 (2023).
[78] F. Buscemi, E. Piccinini, L. Vandelli, F. Nardi, A. Padovani, B. Kaczer, D. Garbin, S. Clima, R. Degraeve, G.S. Kar, F. Tavanti, A. Slassi, A. Calzolari, L. Larcher. IEEE Trans. Electron Dev., **70**, 1808 (2023).
[79] T. Ravsher, R. Degraeve, D. Garbin, A. Fantini, S. Clima, G.L. Donadio, S. Kundu, H. Hody, W. Devulder, J. Van Houdt, V. Afanas'ev. Proc. Int. Electron Dev. Meet., **18**, 2300415 (2021).
[80] S. Hong, H. Choi, J. Park, Y. Bae, K. Kim, W. Lee, S. Lee, H. Lee, S. Cho, J. Ahn, S. Kim. Proc. Int. Electron Dev. Meet. (San Francisco, California, USA, 2022) p. 18.
[81] T. Ravsher, D. Garbin, A. Fantini, R. Degraeve, S. Clima, G.L. Donadio, S. Kundu, H. Hody, W. Devulder, G. Potoms, T. Peissker. Phys. Status Solidi RRL, **18**, 2300415 (2024).
[82] H.J. Sung, M. Choi, Z. Wu, H. Chae, S. Heo, Y. Kang, B. Koo, J.B. Park, W. Yang, Y. Park, Y. Ham. Adv. Sci., **11**, 2408028 (2024).
[83] J. Park. Electronics, **9**, 1414 (2020).
[84] C. Li, M. Hu, Y. Li, H. Jiang, N. Ge, E. Montgomery, J. Zhang, W. Song, N. Dávila, C.E. Graves, Z. Li, J.P. Strachan, P. Lin, Z. Wang, M. Barnell, Q. Wu, R.S. Williams, J.J. Yang, Q. Xia. Nature Electronics, **1**, 52 (2018). DOI: 10.1038/s41928-017-0002-z
[85] A.I. Iliasov, A.V. Emelyanov, V.V. Rylkov, A.N. Matsukatova, E.V. Kukueva, I.D. Kuchumov, P.A. Forsh, A.V. Sitnikov, V.A. Demin, P.K. Kashkarov, M.V. Kovalchuk. J. Phys. D: Appl. Phys., **58**, 365305 (2025).
[86] P.E. Lvov, R.T. Sibatov, R.M. Ryazanov, D.V. Novikov. Materials Today Commun., **38**, 108464 (2024).
[87] C.D. Wright, L. Wang, M.M. Aziz, J.A.V. Diosdado, P. Ashwin. Phys. Status Solidi B, **249**, 1978 (2012).
[88] A.S. Ilyin, A.N. Matsukatova, M.N. Martyshov, A.V. Yemelyanov, V.V. Rylkov, V.A. Demin, P.A. Forsh, P.K. Kashkarov, M.V. Kovalchuk. UFN, accepted for publication. DOI: 10.3367/UFNr.2025.09.040037
[89] Abu Sebastian, M. Le Gallo, E. Eleftheriou. J. Phys. D: Appl. Phys., **52**, 443002 (2019).
[90] M. Rutten, M.E. Kaes, A. Albert, M.Wuttig. Sci. Rep., **5**, 1 (2015).
[91] M. Suri, D. Garbin, O. Bichler, D. Querlioz, D. Vuillaume, C. Gamrat, B. De Salvo. *2013 IEEE ACM Int.Symp. on Nanoscale Architectures* (NANOARCH), (Brooklyn, N.Y., USA, 2013) p. 140.
[92] E. Trusov, Y. Vorobyov, A. Ermachikhin, L. Al-Khadge, A. Yakubov, D. Terekhov, P. Lazarenko, S. Kozyukhin. J. Phys. D: Appl. Phys., **58**, 305104 (2025).
[93] D. Ielmini, A.L. Lacaita, D. Mantegazza. IEEE Trans. Electron Dev., **54**, 308–315 (2007).
[94] A. Pirovano, A.L. Lacaita, A. Benvenuti, F. Pellizzer, R. Bez. IEEE Trans. Electron Dev., **51**, 714 (2004).
[95] I.V. Karpov, M. Mitra, D. Kau, G. Spadini, Y.A. Kryukov,V.G. Karpov. J. Appl. Phys., **102**, 124503 (2007).
[96] M. Mitra, Y. Jung, D.S. Gianola, R. Agarwal. Appl. Phys. Lett., **96**, 222111 (2010).
[97] M.L. Gallo, D. Krebs, F. Zipoli, M. Salinga, A. Sebastian. Adv. Electron. Mater., **4** (9), 1700627 (2018).
[98] X. Wang, R. Wang, S. Sun, D. Xu, C. Nie, Z. Zhou, C. Wen, J. Zhang, R. Chu, X. Shen, W. Zhou, Z. Song, J.-J. Wang, E. Ma, W. Zhang. Nature Mater. (2025). DOI: 10.1038/s41563-025-02361-0
[99] A.I. Musorin, A.S. Shorokhov, A.A. Chezhegov, T.G. Baluyan, K.R. Safronov, A.V. Chetvertukhin, A.A. Grunin, A.A. Fedyanin. UFN, **193**, 1284 (2023). (in Russian).
[100] C. Lian, Ch. Vagionas, Th. Alexoudi, N. Pleros, N. Youngblood, C. Ríos. Nanophotonics, **11** (17), 3823 (2022).

[101] W.H.P. Pernice, H. Bhaskaran. Appl. Phys. Lett., **101**, 171101 (2012).
[102] T. Li, Y. Li, Y. Wang, Y. Liu, Y. Liu, Z. Wang, R. Miao, D. Han, Z. Hui, W. Li. Nanomaterials, **13**, 1756 (2023).
[103] X. Chen, Y. Xue, Y. Sun, J. Shen, S. Song, M. Zhu, Z. Song, Z. Cheng, P. Zhou. Adv. Mater., **35**, 2203909 (2023).
[104] Z. Cheng, C. Ríos, W.H.P. Pernice, C.D. Wright, H. Bhaskaran. Sci. Adv., **3**, e1700160 (2017).
[105] X. Chen, Y. Xue, Y. Sun, J. Shen, S. Song, M. Zhu, Z. Song, Z. Cheng, P. Zhou. Adv. Mater., **35** (37), 2203909 (2023).
[106] P. Lazarenko, V. Kovalyuk, P. An, A. Prokhodtsov, A. Golikov, A. Sherchenkov, S. Kozyukhin, I. Fradkin, G. Chulkova, G. Goltsman. APL Mater., **9** (12), 121104 (2021).
[107] R. Sawant, A. Albanese, A. Rogemont, G. Gonzalez-Cortes, Y. Brlé, L. Karam, J.-B. Jager, S. Malhouitre, B. Charbonnier, A. Coillet, P. Noé, B. Cluzel. Adv. Optical Mater., **13**, e00775 (2025).
[108] Y. Fei, Y. Xu, Y. Dong, B. Zhang, Y. Ni. Appl. Optics, **62** (24), 6499 (2023).
[109] V.V. Ionin, A.V. Kiselev, A.A. Burtsev, V.A. Mikhalevsky, N.N. Eliseev, I.M. Asharchuk, V.I. Sokolov, A.A. Lotin. Appl. Phys. Lett., **119** (8), 081105 (2021).
[110] M. Stegmaier, C. Ríos, H. Bhaskaran, W.H.P. Pernice. ACS Photonics, **3** (5), 828(2016).
[111] W. Zhou, N. Farmakidis, J. Feldmann, X. Li, J. Tan, Y. He, C.D. Wright, W.H.P. Pernice, H. Bhaskaran. MRS Bulletin, **47**, 502 (2022).
[112] M. Stegmaier, C. Ríos, H. Bhaskaran, C.D. Wright, W.H.P. Pernice. Adv. Opt. Mater., **5**, 1600346 (2017).
[113] P. Lazarenko, V. Kovalyuk, P. An, S. Kozyukhin, V. Takáts, A. Golikov, V. Glukhenkaya, Y. Vorobyov, T. Kulevoy, A. Prokhodtsov, A. Sherchenkov, G. Goltsman. Acta Mater., **234**, 117994 (2022).
[114] S.A. Kozyukhin, P.I. Lazarenko, A.I. Popov, I.L. Eremenko. Russian Chem. Rev., **91**, 9 (2022).
[115] N. Bala, B. Khan, K. Singh, P. Singh, A.P. Singh, A. Thakur. Mater. Adv., **4**, 747 (2023).
[116] M. Delaney, I. Zeimpekis, D. Lawson, D.W. Hewak, O.L. Muskens. Adv. Funct. Mater., **30** (36), e2002447 (2020).
[117] X.B. Li, N.K. Chen, X.P. Wang, H.B. Sun. Adv. Funct. Mater., **28** (44), 1803380 (2018).
[118] P. Lazarenko, V. Kovalyuk, P. An, A. Prokhodtsov, A. Golikov, A. Sherchenkov, S. Kozyukhin, I. Fradkin, G. Chulkova, G. Goltsman. APL Mater., **9**, 121104 (2021).
[119] E. Menshikov, P. Lazarenko, V. Kovalyuk, S. Dubkov, N. Maslova, A. Prokhodtsov, A. Vorobyov, S. Kozyukhin, G. Goltsman, I.S. Sinev. ACS Appl. Mater. Interfaces, **16** (29), 38345 (2024).
[120] M. Wuttig, H. Bhaskaran, T. Taubner. Nature Photonics, **126**, 465 (2017).
[121] S. Wen, X. Meng, M. Jiang, Y. Wang. Sci. Rep., **8** (1), 1 (2018).
[122] A.A. Gavdush, G.A. Komandin, V.V. Bukin, D.S. Ponomarev, L. Tan, W. Huang, Q. Shi. J. Appl. Phys., **134**, 085103 (2023).
[123] J. Faneca, T.D. Bucio, F.Y. Gardes, A. Baldycheva. Appl. Phys. Lett., **116** (9) (2020).
[124] S. Seliverstov, S. Svyatodukh, A. Kozhukhovsky, D. Fudin, P. Lazarenko, D. Terekhov, A. Prokhodtsov, A. Nevzorov, E. Kitsyuk, A. Prikhodko, A. Shurakov, V. Kovalyuk, G. Goltsman. Optical Mater., **167**, 117216 (2025).
[125] I. Chakraborty, G. Saha, K. Roy. Phys. Rev. Appl., **11**, 014063 (2019).
[126] Z. Cheng, C. Ríos, W.H.P. Perniceet, C.D. Wright, H. Bhaskaran. Sci. Adv., **3** (9), e1700160 (2017).
[127] J. Feldmann, N. Youngblood, D. Wright, H. Bhaskaran, W.H.P. Pernice. Nature, **569**, 208 (2019).
[128] J. Feldmann, N. Youngbloo, M. Karpov, H. Gehring, X. Li, M. Stappers, M. Le Gallo, X. Fu, A. Lukashchuk, A.S. Raja, J. Liu, C.D. Wright, A. Sebastian, T.J. Kippenberg, W.H.P. Pernice, H. Bhaskaran. Nature, **589**, 52 (2021).
[129] N. Farmakidis, B. Dong, H. Bhaskaran. Nature Rev. Electr. Eng., **1**, 358 (2024).
[130] D.V. Christensen, R. Dittmann, B. Linares-Barranco, A. Sebastian, M. Le Gallo, A. Redaelli, S. Slesazeck, T. Mikolajick, S. Spiga, S. Menzel, I. Valov, G. Milano, C. Ricciardi, S.-J. Liang, F. Miao et al. Neuromorph. Comput. Eng., **2** (2), 022501 (2022).
[131] P. Prabhathan, K.K.V. Sreekanth, J. Teng, J.H. Ko, Y.J. Yoo, H.-H. Jeang, Y. Lee, S. Zhang, T. Cao, C.-C. Popescu, B. Mills, T. Gu, Z.R. Chen, Y. Tong, Y. Wang, Q. He, Y. Lu, Z. Liu, H. Yu, A. Mandal, Y. Cui et al. iScience, **26** (10), 107946 (2023).
[132] M. Xu, X. Mai, J. Lin, W. Zhang, Y. Li, Y. He, H. Tong, X. Hou, P. Zhou, X. Miao. Adv. Funct. Mater., **30**, 2003419 (2020).
[133] L. Wang, S.R. Lu, J. Wen. Nanoscale Res. Lett., **12**, 347 (2017).
[134] S.A. Kozyukhin, P.I. Lazarenko, A.I. Popov, I.L. Eremenko. Russian Chem. Rev., **91**, 9 (2022).
[135] C. Li, R. Pan, C. Gu, H. Guo, J. Li. Adv. Sci., **11**, 2306344 (2024).
[136] G.S. Sarwat, M. Le Gallo, A. Sebastian. Chem. Rev., **125**, 5163 (2025).
[137] B. Gholipour, A. Karvounis, J. Yin, C. Soci, K.F. MacDonald, N.I. Zheludev. NPG Asia Materials, **10**, 533 (2018).
[138] Y. Meng, T. Cao, Y. Long. J. Appl. Phys., **128**, 140904 (2020).
[139] C. Galarreta, I. Sinev, A.M. Alexeev, P. Trofimov, K. Ladutenko, S. Carrillo, E. Gemo, A. Baldycheva, J. Bertolotti, C.D. Wright. Optica, **7** (5), 476 (2020).
[140] C.R. De Galarreta, A.M. Alexeev, Y.-Y. Au, M. Lopez-Garcia, M. Klemm, M. Cryan. Adv. Funct. Mater., **28** (10), 1704993 (2018). DOI: 10.1002/adfm.201704993
[141] A.V. Pogrebnyakov, J.A. Bossard, J.P. Turpin, J.D. Musgraves, H.J. Shin, C. Rivero-Baleine et al. Opt. Mater. Express, **8** (8), 2264 (2018). DOI: 10.1364/OME.8.002264
[142] Cao, C. Wei, R.E. Simpson, L. Zhang, M.J. Cryan. Sci. Rep., **4**, 3955 (2014). DOI: 10.1038/srep03955
[143] A.I. Solomonov, O.M. Kushchenko, K.I. Kasyanova, S.B. Isaeva, I.I. Shishkin, D.Y. Terekhov, P.I. Lazarenko, M.V. Rybin, S.S. Baturin, A.D. Sinelnik. Appl. Mater. Today, **37**, 102135 (2024).
[144] T. Kunkel, Y. Vorobyov, M. Smayev, P. Lazarenko, A. Romashkin, S. Kozyukhin. Mater. Sci. Semicond. Proc., **139**, 106350 (2022).
[145] A. Sajjad, O. Hemmatyar, M. Taghinejad, H. Taghinejad, A. Krasnok, A.A. Eftekhar, C. Teichrib, S. Deshmukh, M.A. El-Sayed, E. Pop, M. Wuttig, A. Alù, W. Cai, A. Adibi. Nature Commun., **13**, 1696 (2022).
[146] W. Dong, H. Liu, J.K. Behera, L. Lu, R.J. Ng, K.V. Sreekanth, X. Zhou, J.K. Yang, R.E. Simpson. Adv. Funct. Mater., **29**, 1806181 (2019).

[147] Z. Yu, J. Zheng, P. Xu, W. Zhang, Y. Wu. IEEE Phot.Technol. Lett., **30**, 250 (2017).
[148] M. Singh, S.K. Raghuwanshi, T. Srinivas. Phys. Lett. A, **383**, 3196 (2019).
[149] Z. Guo, X. Yang, F. Shen, Q. Zhou, J. Gao, K. Guo. Sci. Rep., **8**, 1 (2018).
[150] Y. Wang, P. Landreman, D. Schoen, K. Okabe, A. Marshall, U. Celano, H.-S.P. Wong, J. Park, M.L. Brongersma. Nature Nanotechnol., **16**, 667 (2021).
[151] Y. Li, J. Luo, X. Li, M. Pu, X. Ma, X. Xie, J. Shi, X. Luo. IEEE Photonics J., **12**, 1 (2020).
[152] C.Y. Hwang, G.H. Kim, J.H. Yang, C.S. Hwang, S.M. Cho, W.J. Lee, J.E. Pi, J.H. Choi, K. Choi, H.O. Kim et al. Nanoscale, **10**, 21648 (2018).
[153] Y. Qu, Q. Li, L. Cai, M. Pan, P. Ghosh, K. Du, M. Qiu. Light: Sci. Appl., **7**, 26 (2018).

Translated by A.Akhtyamov